

Journal of Experimental Botany, Vol. 72, No. 11 pp. 4161–4179, 2021 doi:10.1093/jxb/erab051 Advance Access Publication 17 February 2021



RESEARCH PAPER

Natural ultraviolet radiation exposure alters photosynthetic biology and improves recovery from desiccation in a desert moss

Jenna T.B. Ekwealor^{1,*,}, Theresa A. Clark², Oliver Dautermann³, Alexander Russell², Sotodeh Ebrahimi², Lloyd R. Stark², Krishna K. Niyogi^{3,4,5} and Brent D. Mishler¹

- ¹ Department of Integrative Biology, and University and Jepson Herbaria, University of California, Berkeley, CA, USA
- ² School of Life Sciences, University of Nevada, Las Vegas, NV, USA
- ³ Department of Plant and Microbial Biology, University of California, Berkeley, CA, USA
- ⁴ Howard Hughes Medical Institute, University of California, Berkeley, CA, USA
- ⁵ Molecular Biophysics and Integrated Bioimaging Division, Lawrence Berkeley National Laboratory, Berkeley, CA, USA
- * Correspondence: jtbe@berkeley.edu

Received 1 December 2020; Editorial decision 26 January 2021; Accepted 1 February 2021

Editor: Karl-Josef Dietz, Bielefeld University, Germany

Abstract

Plants in dryland ecosystems experience extreme daily and seasonal fluctuations in light, temperature, and water availability. We used an *in situ* field experiment to uncover the effects of natural and reduced levels of ultraviolet radiation (UV) on maximum PSII quantum efficiency (F_v/F_m) , relative abundance of photosynthetic pigments and antioxidants, and the transcriptome in the desiccation-tolerant desert moss *Syntrichia caninervis*. We tested the hypotheses that: (i) *S. caninervis* plants undergo sustained thermal quenching of light [non-photochemical quenching (NPQ)] while desiccated and after rehydration; (ii) a reduction of UV will result in improved recovery of F_v/F_m ; but (iii) 1 year of UV removal will de-harden plants and increase vulnerability to UV damage, indicated by a reduction in F_v/F_m . All field-collected plants had extremely low F_v/F_m after initial rehydration but recovered over 8 d in lab-simulated winter conditions. UV-filtered plants had lower F_v/F_m during recovery, higher concentrations of photoprotective pigments and antioxidants such as zeaxanthin and tocopherols, and lower concentrations of neoxanthin and Chl *b* than plants exposed to near natural UV levels. Field-grown *S. caninervis* underwent sustained NPQ that took days to relax and for efficient photosynthesis to resume. Reduction of solar UV radiation adversely affected recovery of F_v/F_m following rehydration.

Keywords: Biological soil crust, desiccation tolerance, maximum PSII quantum efficiency (F_v/F_m), Mojave Desert, moss, non-photochemical quenching (NPQ), photosynthetic efficiency, photosynthetic pigments, *Syntrichia caninervis*, UV tolerance.

Introduction

Drylands represent the largest terrestrial biome, accounting for at least 35% of Earth's land mass (Middleton and Thomas, 1992; Peel et al., 2007). These ecosystems experience extreme daily and seasonal fluctuations in light, temperature, and water availability, often concomitantly. Interaction between extreme environmental conditions such as low water availability and high light represents a particular challenge for plants. To survive dry periods, many dryland bryophytes and a smaller number of vascular plants have evolved vegetative desiccation tolerance, defined as the ability to equilibrate to dry air and resume metabolic activity after rehydration (Gaff, 1977; Proctor et al., 2007; Stark, 2017). Yet, while desiccation tolerance allows these plants to survive dry periods by limiting metabolic activity to periods of adequate moisture availability, this adaptation implicates long periods of exposure to high light intensity during full sun, including unusable photosynthetically active radiation (PAR) and direct ultraviolet radiation (UV), both of which may be harmful.

Plants may respond to radiation stresses via photosynthetic pigments and antioxidants (Demmig-Adams and Adams, 1996; Frohnmeyer and Staiger, 2003; Li et al., 2009; Liguori et al., 2017). During periods of exposure to high light, excess energy absorbed by chlorophylls forms reactive oxygen species (ROS), which react with and damage the sensitive molecular machinery (Li et al., 2009). Plants, therefore, face the trade-off of maximizing light absorbance for use in photosynthesis while also providing adequate photoprotection to minimize ROS damage; desert mosses need to balance these requirements both when metabolically active and when desiccated. One of the major photoprotective mechanisms in plants is the dissipation of excess light energy as heat, a set of processes collectively known as non-photochemical quenching (NPQ; Müller et al., 2001; Ruban, 2016; Malnoë, 2018). Light energy absorbed by chlorophylls can follow one of several competitive pathways: transformation into chemical energy via photochemistry and photosynthetic electron transport, transfer to oxygen to form ROS, re-emission as fluorescence from excited chlorophyll molecules, or dissipation as heat via NPQ. This last pathway of heat dissipation functions like a 'safety valve' for photosynthesis (Niyogi, 2000) that prevents or reduces damage from excess light.

Some carotenoids function in NPQ and directly quench ROS such as singlet oxygen (Baroli et al., 2000). Importantly, a strong correlation between zeaxanthin accumulation and a rapidly inducible form of NPQ, known as energy-dependent quenching (qE; Horton et al., 1996; Niyogi, 2000), has been demonstrated in several tracheophyte species (Demmig-Adams, 1990; Demmig-Adams and Adams, 1996). Sustained NPQ mechanisms, often referred to as photoinhibitory quenching (qI), result in a decrease in the quantum efficiency of photosynthesis and can also be associated with zeaxanthin, though possibly through a different, pH-independent mechanism (Verhoeven et al., 1996). Desert plants might be expected to undergo the qE form of NPQ for diurnal fluctuations in light intensity as well as qI or other sustained NPQ forms, such as qH (Malnoë, 2018), to deal with seasonal changes in light. Indeed, desiccation-tolerant mosses have been shown to exhibit strong, sustained mechanisms of NPQ after exposure to high light or desiccation (Yamakawa et al., 2012; Yamakawa and Itoh, 2013).

In addition to changes in overall light intensity, plants, like other organisms, are sensitive to UV radiation, an important stressor that plants must cope with in nature (Jansen et al., 1998; Wolf et al., 2010). An array of cellular components are damaged by absorption of UV-B radiation (280-315 nm), including components of the photosynthetic apparatus (Teramura and Sullivan, 1994; Jansen et al., 1998). UV-B triggers the production of carotenoids (Middleton and Teramura, 1993), and some of the same high-light photoprotective mechanisms can also protect plants from UV radiation. For example, it was demonstrated that zeaxanthin contributes to UV stress protection and damage prevention in tobacco (Götz et al., 2002). Additionally, some plants have evolved UV-absorbing chemical sunscreens such as flavonoids that reduce the amount of UV reaching sensitive molecules (Tohge and Fernie, 2017).

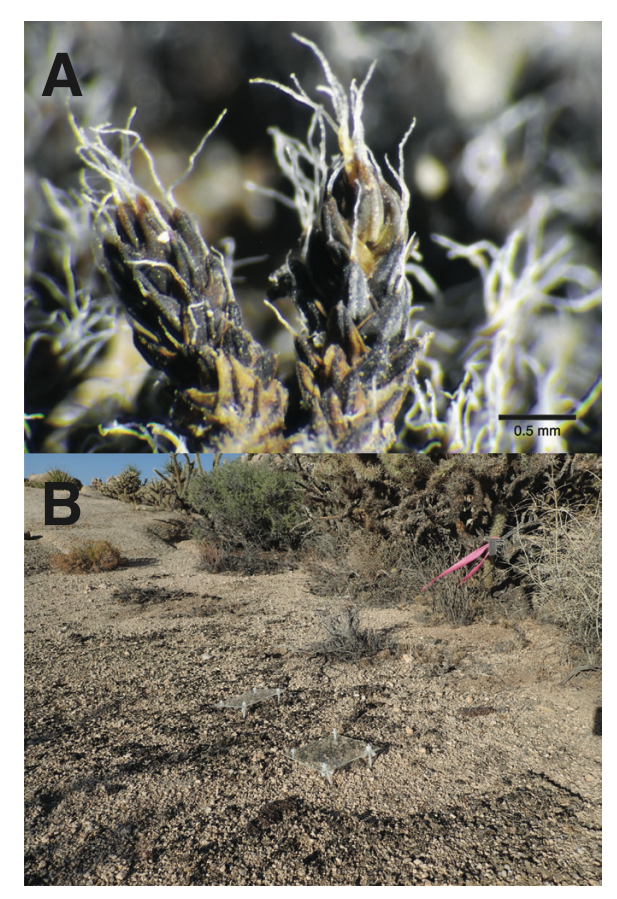
Exposure to UV radiation does not always yield a negative effect for photosynthetic organisms, however. Recently there has been a paradigm shift in understanding UV as a regulatory signal rather than solely a stressor, as UV perception is involved in critical metabolic functions (Rozema et al., 1997; Davey et al., 2012; Hideg et al., 2013; Morales et al., 2013; Singh et al., 2014; Williamson et al., 2014; Neugart and Schreiner, 2018). Researchers have begun to instead classify UV radiation as a 'eustress' (Hideg et al., 2013). In this framework, UV-B is understood to stimulate a state of alert that includes activation defenses, especially if the radiation is experienced in small doses. For example, UVR8, the UV-B receptor in plants, mediates the accumulation of transcripts encoding early lightinducible proteins (ELIPs) (Singh et al., 2014), which function in photoprotection (Hutin et al., 2003). Furthermore, low doses of UV radiation can induce protective responses that increase a plant's tolerance to other abiotic and biotic stressors (Frohnmeyer and Staiger, 2003). For instance, ELIPs are also important for desiccation tolerance in resurrection plants (Zeng, 2002; Oliver et al., 2004; Van Buren et al., 2019).

Although many mosses are found in cool, low-light environments, several species are abundant in drylands where they are common and important members of biological soil crusts (biocrusts). Biocrusts are complex communities of bryophytes, lichens, fungi, cyanobacteria, and other microorganisms living on the surface of soil in drylands (Belnap et al., 2003). These communities provide critical ecosystem services such as reducing erosion, increasing soil fertility and water infiltration, and even facilitating germination of native seeds while reducing germination of large-appendaged exotic seeds (Harper and

Belnap, 2001; Belnap, 2002, 2006; Belnap et al., 2003; Hawkes, 2004; Li et al., 2005; Su et al., 2007). Mosses play important roles in biocrusts, such as contributing to both soil stability via rhizoids and soil formation via capture of nutrient-rich fine particles (Seppelt et al., 2016). Moreover, in some dryland ecosystems, biocrust mosses control the overall carbon balance by reaching peak photosynthetic activity during winter months when surrounding shrubs are dormant (Zaady et al., 2000; Jasoni et al., 2005). However, Mojave Desert mosses are faced with being quiescent during hot, dry summers and are thus unable to use any of the intense solar radiation for photosynthesis (Stark, 2005). Furthermore, while many plants have morphological mechanisms to reduce absorption of excess light, such as altering leaf angle or the production of a waxy cuticle, mosses both lack thick cuticles (Jeffree, 2007) and are unable to alter leaf angle once desiccated. Although their dry state is often a curled state, thought to be a protective adaptation for minimizing light absorption (Zotz and Kahler, 2007), it may not alone be enough to protect desert mosses from the long-term excess light and intense UV radiation they face while quiescent.

Studies on UV protection in mosses have been limited, with most focus on Antarctic mosses and UV-B supplementation in greenhouses or growth chambers (Gwynn-Jones et al., 1999; Searles et al., 1999, 2001; Lud et al., 2002; Martínez-Abaigar et al., 2003; Newsham, 2003; Green et al., 2005; Núñez-Olivera et al., 2005; Robinson et al., 2005; Dunn and Robinson, 2006; Björn, 2007; Turnbull et al., 2009). Thus, there is a need for a better understanding of the effects of natural levels of UV radiation in a field setting. While nearly all mosses tested in nature appear to be minimally damaged by ambient UV levels (Boelen et al., 2006), in some species UV protection appears to be physiologically constitutive and in others it is plastic. For example, the Antarctic mosses Ceratodon purpureus and Bryum subrotundifolium exhibit sun forms that are tolerant to UV, and shade forms that are not but can be acclimated to UV within a week in natural sunlight (Green et al., 2005). On the other hand, in the mosses Sanionia uncinata, Chorisodontium aciphyllum, Warnstorfia sarmentosa, and Polytrichum strictum, also from Antarctica, UV-B-absorbing compounds are not induced by enhanced UV-B radiation (Boelen et al., 2006). Similarly, field-collected plants of Syntrichia ruralis, a dryland moss, were unaffected by supplemental UV-B radiation, based on chlorophyll fluorescence (Takács et al., 1999; Csintalan et al., 2001). Yet while this species appears to have sufficient UV protection, it is unclear whether it is constitutive or inducible, whether with UV or another environmental cue. Studies have shown that UV tolerance correlates with desiccation tolerance (Takács et al., 1999), and that desiccation itself confers extra protection from UV in two Antarctic mosses (Turnbull et al., 2009). Both habitat and genetics are strong predictors of UV tolerance in bryophytes, but there is much within- and among-genera variability (Hespanhol et al., 2014). Thus, the need to study each species in its own environment is critical to understanding how UV is tolerated in nature.

The desert moss Syntrichia caninervis is a highly desiccationtolerant (Proctor et al., 2007; Stark, 2017) important member of western North American dryland biocrust communities, including in the Mojave Desert (Stark et al., 1998; Bowker et al., 2000; Coe et al., 2012; Antoninka et al., 2016; Seppelt et al., 2016). This species frequently forms continuous or semicontinuous carpets in exposed, intershrub desert soil crusts, and tolerates high levels of solar radiation while dry. Interestingly, mature shoots of S. caninervis develop a dark brown or black coloration in nature (Fig. 1A), but remain bright green when grown in dim, artificial laboratory light (personal observation), suggesting a plastic pigment accumulation reaction in response



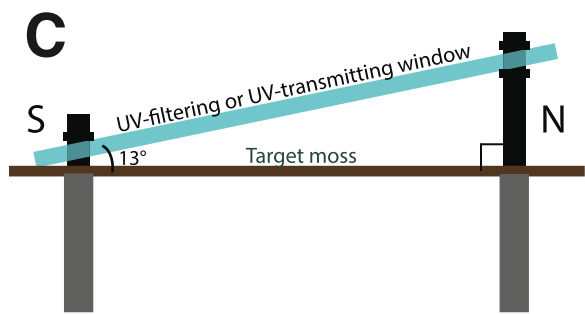


Fig. 1. Natural Syntrichia caninervis. (A) Desiccated S. caninervis shoots. (B) Experimental set-up, showing UV-filtering and UV-transmitting windows over S. caninervis cushions in the Mojave Desert. (C) Schematic of field window design.

4164 | Ekwealor *et al.*

to light exposure. Accumulation of dark pigmentation varies in nature, too. *Syntrichia caninervis* plants are greener in very low-light microhabitats (Ekwealor and Fisher, 2020) and when UV is filtered out of natural sunlight (Ekwealor, 2020). This apparent 'suntan' pattern suggests the possibility of an adaptive response for UV protection, though that function has not yet been tested in *S. caninervis*.

To this end, we conducted an integrated, four-part experiment to test how desert mosses withstand solar radiation while quiescent under natural and extreme fluctuations in climate and solar radiation characteristic of the Mojave Desert. We deployed a year-long, controlled UV reduction manipulation on 20 in situ microsites of S. caninervis to test the hypotheses that: (i) natural S. caninervis plants undergo sustained NPQ while desiccated and after rehydration; (ii) if UV radiation is a stressor, then a reduction of natural levels of UV will result in improved recovery of maximum PSII quantum efficiency (F_v/F_m) ; but (iii) 1 year of UV removal will de-harden plants and thus increase vulnerability to UV damage, indicated by a reduction in F_v/F_m after a laboratory UV treatment. In order to better understand the mechanisms of photoprotection, UV tolerance, and recovery from desiccation, we measured the relative abundance of photosynthetic pigments and antioxidants in field-manipulated plants, and quantified differential transcript

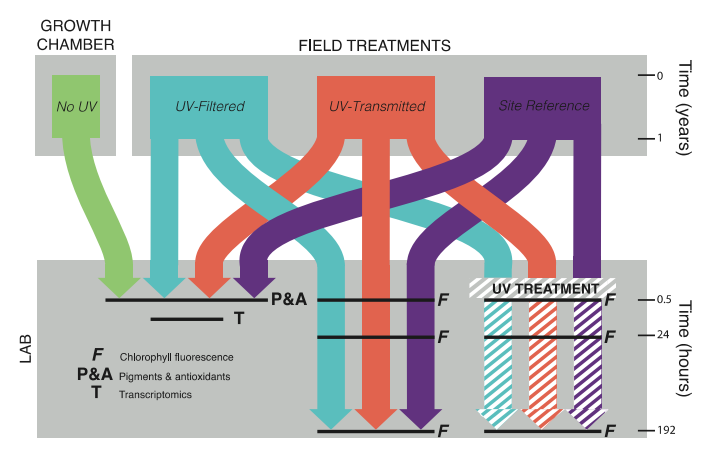


Fig. 2. Integrated experimental design. The top panel represents Syntrichia caninervis growth conditions, including field treatments and growth chamber cultures. UV-Filtered refers to plants that had UV-filtering windows in situ for 1 year. UV-Transmitted represents plants that had UV-transmitting windows installed, and Site Reference represents unmanipulated field-collected samples. Conditions in the field experiment included ambient sunlight and natural desiccation-hydration cycles, while conditions in the growth chamber included low light and continuous hydration. Samples from each growth condition were used in various laboratory experiments and measurements, including a simulated winter recovery from desiccation (indicated with the 0.5-192 h time scale; hours post-rehydration), measurement of relative abundance of photosynthetic pigments and antioxidants (indicated with 'P&A'), chlorophyll fluorescence assays (indicated with 'F'), and transcriptomics (indicated with 'T'). Striped arrows indicate that field-manipulated, desiccated plants received an in-laboratory UV treatment to test for de-hardening and PSII protection from UV radiation.

abundance on UV-reduced plants and controls. Finally, to understand the effects of the high light and desiccating natural environment on the pigment and antioxidant profiles, we compared field-collected, unmanipulated *S. caninervis* plants with those cultured in a laboratory growth chamber.

Materials and methods

Code and data availability

Analyses and graphical visualizations were performed in R (R Core Team, 2019) unless otherwise stated using the packages lubridate (Grolemund and Wickham, 2011), rstatix (Kassambara, 2020*a*), tidyverse (Wickham *et al.*, 2019), dplyr (Wickham *et al.*, 2020), ggbiplot (Vu, 2011), ggplot2 (Wickham, 2016), Rmisc (Hope, 2013), and ggpubr (Kassambara, 2020*b*). The R function script, ibutton.functions. R (https://github.com/aammd/ibutton.functions), was used to process ibutton temperature and relative humidity data. The analysis code and pigment, antioxidant, fluorescence, and microclimate data from this study are openly available on GitHub at: https://github.com/jenna-tb-ekwealor/syntrichia_field_UV. Raw RNAseq data is available on the NCBI GenBank SRA under BioProject PRJNA704617.

Study site and samplings

The study was conducted in the southwestern Mojave Desert at the Sweeney Granite Mountains Desert Research Center, an ecological reserve of the University of California Natural Reserve System, using an integrated four-part field and laboratory design (Fig. 2). Experimental treatments and sampling took place within a cove in the Granite Mountains (~1360 m elevation) dominated by *Cylindropuntia acanthocarpa*, *C. echinocarpa*, *Larrea tridendata*, and *Yucca schidigera* (34.7849°N, 115.6620°W). The terrain in this area is relatively flat with some gentle slopes, and is characterized by abundant, large granitic boulders and seasonal washes. The climate is arid, with a mean annual precipitation of 217 mm, a mean summer (May through October) daily high temperature of 29 °C, a mean summer daily low of 18 °C, a mean winter (November through April) daily high of 16 °C, and a mean winter daily low of 6 °C (data from UC Sweeney Granite Mountains Desert Research Center, Sweeney Granite Reserve Weather Station, RGSC1, 34.78°N, 115.65°W, 1304 m elevation).

To test for the effects of prolonged reduction of UV radiation in a natural habitat, UV-filtering and UV-transmitting windows were installed over S. caninervis plants in situ. In June 2018, twenty 12.7 cm×12.7 cm (5"×5") UV-filtering windows (Fig. 1B, C), 3.175 mm (1/8") thick (OP-3 acrylic, Acrylite, Sanford, ME, USA), were installed over target S. caninervis cushions at the study site (a voucher specimen, Ekwealor 015, has been deposited in the UC herbarium). The UV-filtering windows transmit ~90% of radiation across the visible spectrum with a sharp drop to ~0% transmittance between 425 nm and 400 nm (www.sdplastics. com/acryliteliterature/1682ACRYLITEOP3techData.pdf). In a paired design, 20 UV-transmitting, but otherwise identical, acrylic windows (Polycast Solacryl SUVT acrylic, Spartech, Maryland Heights, MO, USA) were placed over target cushions located within 1 m of their UV-filtering counterpart (Fig. 1B). These UV-transmitting windows transmit at least 90% across the visible and UV-A/B spectrum and then drop to near 0% transmittance between 275 nm and 250 nm (www.polymerplastics.com/ transparents_uvta_sheet.shtml). Both types of windows transmit 90% of PAR (400-700 nm). Additionally, three pairs of windows were installed for microclimate measurements (see below). All windows were installed using #8-32 threaded nylon legs so that each window was nearly flush with the ground on the south edge and ~2.5 cm off the ground on the north edge, creating an approximately 13° angle with the soil surface.

Window installations were monitored and re-secured monthly until sample collection in June 2019. At that time, one UV-filtering window had been lost to weather and that pair was excluded from downstream analyses. Although it is not possible to determine when the mosses were last naturally hydrated in their habitat, it had rained 1.6 cm 1 month prior to collection, at which time samples were not observed to be hydrated beneath the windows. Cushions were collected dry using 9 cm diameter culture dishes from each of the remaining 19 pairs along with an additional third, unmanipulated site reference (within 1 m of the window pair). This latter 'site reference' was used to test for effects of a window treatment per se. Specimens were stored dry (Fig. 1A) and in the dark until analyses.

Light measurements

PAR and UV-A/B radiation (250-400 nm) were measured under windows and at nearby unmanipulated site reference mosses in April 2019 using LightScout UV and Quantum Sensors and the LightScout Sensor Reader (Spectrum Technologies, Aurora, IL, USA). Light under each pair of windows was measured at the same time, though measurements of all pairs were completed over the course of 2 h. Data were first tested for normality with the Shapiro-Wilk test (Shapiro and Wilk, 1965). Differences in PAR between field treatments were tested for with twotailed paired Student's t-tests, and differences in UV were tested for with Wilcoxon signed-rank tests (Wilcoxon, 1945). Significance was adjusted with the Benjamini and Hochberg (BH) correction (Benjamini and Hochberg, 1995) to account for the false discovery rate of multiple tests (Jafari and Ansari-Pour, 2019).

In addition to PAR and UV point measurements, total light intensity was monitored under three UV-filtering and UV-transmitting window pairs every 30 min for 4 months from February 2019 until 3 d before sample collection in June 2019 with an Onset HOBO Pendant Temperature/Light (relative light intensity from 0 to 320 000 lux) Logger (UA-002, Onset Computer Corporation, Bourne, MA, USA). Data were summarized to mean daily highs and lows per month for each treatment per microsite pair. Mean daily highs and lows per month were tested for treatment effects with a one-way repeated measures ANOVA for each pair.

Microclimate

In order to quantify the effects of the window treatments on the microclimate, climate sensors were deployed under three pairs of windows and at nearby soil surface mosses. These windows were installed specifically for this purpose and moss samples were not collected from them. To log relative humidity every 5 min, iButton hygrochrons (Maxim Integrated, San Jose, CA, USA) were deployed under three pairs in winter (February) and one pair in summer (September) 2019 for a period of 4 d and 2 d, respectively. In September, an iButton hygrochron was also used to measure the relative humidity of a nearby (within 1 m of windows) unmanipulated site reference moss cushion. Relative humidity data from iButtons were summarized to mean daily highs and lows per site and by treatment (UV-filtered, UV-transmitted, plus site reference for summer) and tested for significance of treatment effects with a one-way repeated measures ANOVA for the winter and summer data sets. Tukey's HSD tests were performed as post-hoc analyses (Tukey, 1949).

Temperature was monitored under three UV-filtering and UV-transmitting window pairs every 30 min for 4 months from February 2019 until 3 d before sample collection in June 2019 with an Onset HOBO Pendant Temperature/Light (relative light intensity from 0 to 320 000 lux) Logger (UA-002, Onset Computer Corporation). Data were summarized to monthly mean daily highs and lows for each treatment and site, and to pooled means across all sites. Mean daily highs and lows for each treatment per site per month were tested for significance of treatment effect with a one-way repeated measures ANOVA.

Laboratory cultures

To understand the effects of the natural environment on the pigment and antioxidant profiles, we compared lab-cultured S. caninervis plants with those collected from the field. Shoots from a previously isolated clone of a S. caninervis herbarium specimen from southern Nevada, USA (Stark NV-107, USA, Nevada, Clark County, Newberry Mts, Christmas Tree Pass; UNLV) were cultivated in a growth chamber set to an 18 h photoperiod (18 °C light, 12 °C dark), at ~30 μmol m⁻² s⁻¹ PAR. Cultures of a single genotype were grown from fragments in lidded 77 m×77 m×97 m Magenta GA-7 plant culture boxes (bioWORLD, Dublin, OH, USA) on 1.2% agar made with an inorganic nutrient solution (Hoagland and Arnon, 1950).

Chlorophyll fluorescence of field-manipulated samples

In order to measure recovery of maximum PSII quantum efficiency (F_v/F_m) and operating PSII quantum efficiency (Φ PSII) over a simulated winter recovery period, chlorophyll fluorescence was determined according to a modified version of the protocol used in Clark (2020) at three time points over 192 h. Ten to fifteen shoots of each specimen were sampled by selecting shoots randomly from each cushion. Shoots were hydrated and quickly assembled into Hansatech FMS/LC darkacclimation leaf clips (Hansatech Instruments, Norfolk, UK) that were modified with a deeper cavity to allow tall moss shoots to stand upright on a small, circular piece of filter paper created with a hole-punch, as described in Clark (2020). This system allows the entire moss 'bouquet' to be easily removed by grabbing the filter paper with forceps, so that the same shoots could be measured in the same orientation across recovery time points.

Immediately after moss bouquet assembly, the clip was closed for 30 min to allow shoots to acclimate to darkness (i.e. PSII reaction centers open). At precisely 30 min, the clip was attached to a Hansatech Pulse-Modulated chlorophyll fluorescence probe (FMS 2, Hansatech Instruments) and fluorescence was measured with the following parameters: actinic light of 150 µmol m⁻² s⁻¹ for 200 s; and a saturation pulse of 3000 µmol m⁻² s⁻¹ for 0.8 s applied before and after actinic light to measure dark- and light-acclimated fluorescence metrics, respectively. Fluorescence was measured three times over 8 d in a recovery series: $T_{0.5}$ (0.5 h post-rehydration), T_{24} (24 h post-rehydration), and T_{192} (192 h post-rehydration). Between recovery measurements, bouquets were recovered in a growth chamber on modified 24-well plates called 'water thrones' as described in Clark (2020), which allowed bouquets to remain hydrated and near 100% relative humidity through a water-wicking system using filter paper and pools of water (Supplementary Fig. S1). The Percival E30B growth chamber (Percival Scientific, Perry, IA, USA) was set to simulate winter recovery conditions consisting of a 10 h photoperiod (12 °C light, 5 °C dark) with 70-85% relative humidity at 150 µmol m⁻² s⁻¹ in which temperature and relative humidity were monitored with an iButton data logger (Maxim Integrated).

Raw fluorescence data were used to calculate F_v/F_m and $\Phi PSII. F_v/F_m$ is equal to $(F_{\rm m}-F_{\rm o})/F_{\rm m}$, where $F_{\rm m}$ is maximal fluorescence in the darkacclimated sample and F_0 is minimal fluorescence in the dark-acclimated sample. $\Phi PSII$ is equal to $(F_{\rm m}' - F_{\rm t})/F_{\rm m}'$, where $F_{\rm m}'$ is maximal fluorescence in the light-acclimated sample and $F_{\rm t}$ is steady-state terminal fluorescence. F_v/F_m and Φ PSII data were first tested for normality with the Shapiro-Wilk test (Shapiro and Wilk, 1965), which revealed nonnormality, and subsequently all $F_{\rm v}/F_{\rm m}$ and $\Phi PSII$ were compared pairwise using Wilcoxon signed-rank tests (Wilcoxon, 1945) at each time point. Significance was adjusted for multiple testing with the BH correction.

Test for UV de-hardening at PSII

To test the hypothesis that UV filtering in situ would de-harden plants and increase vulnerability to subsequent UV exposure while dry, plants

4166 | Ekwealor et al.

from all three field treatments were subjected to a laboratory UV exposure-recovery assay. An additional 10-15 shoots per sample were randomly selected from the field samples and given a UV-A/B treatment while dry. Samples were placed under four T8 reptile bulbs (ReptiSun 10.0 UVB, Zoo Med Laboratories Inc., San Luis Obispo, CA, USA) in culture dishes covered by UV-transmitting acrylic (Polycast Solacryl SUVT acrylic, Spartech) to filter out UV-C wavelengths, which, in nature, are absorbed by the earth's atmosphere. Lamps were placed 2.5 cm from specimens for UV-A/B flux of 80 µmol m⁻² s⁻¹, PAR of 160 µmol m⁻² s⁻¹, and UV-B fluence rate of 0.36 mW cm⁻² for 14 h (rotated once during treatment) with a fan to circulate air under the lamp. UV-B fluence was measured at several locations under the lamps with a handheld radiometer that was last calibrated in 2014 and independently evaluated in 2016 (SKU 430, Apollo Display Meter, Skye Instruments Ltd, Llandrindod Wells, UK) and a UV-B sensor that was covered with the same UV-transmitting acrylic. Temperature and relative humidity were monitored with an iButton data logger (Maxim Integrated; 26 °C mean temperature, σ =1.1 °C, 19% mean relative humidity, σ =1.4%). After UV treatment, shoots were prepared for an 8 d chlorophyll fluorescence recovery series as above. To test laboratory UV effects, we compared these laboratory-treated samples with their respective field subsets (UV-filtered, transmitted, and site reference) at each time point (T_{0.5}, T₂₄, and T₁₉₂) using Wilcoxon signed-rank tests on F_v/F_m and $\Phi PSII$.

Photosynthesis pigment and antioxidant content

To explore potential photoprotective responses to in situ UV exposure, the relative abundance of eight pigments and antioxidants was measured in field samples at the end of the 1 year study. Pigment and tocopherol content were quantified by HPLC in at least three biological replicates for each of the 57 field samples for a total of 188 HPLC measurements. Approximately 5 mg (about five shoots) of dry, soil-free plant material was collected from each field triplicate (UV-filtered, transmitted, and site reference) and homogenized in 100% acetone using a FastPrep-24 5G bead beater (MP Biomedicals, Irvine, CA, USA). Additionally, 5-10 shoots of lab-cultured S. caninervis were prepared in at least triplicate. After homogenization in acetone, samples were centrifuged at 14 000 gfor 30 s. Supernatants were passed through a 0.45 µm nylon filter (part F2504-1, ThermoFisher Scientific, Waltham, MA, USA) prior to injection of 25 µl onto a ProntoSIL 200-5-C30, 5.0 µm, 250 mm×4.6 mm column equipped with a ProntoSIL 200-5-C30, 5.0 µm, 20 mm×4.0 mm guard column (Bischoff Analysetechnik, Leonberg, Germany) following the HPLC method and gradient conditions of Dautermann et al. (2020). Tocopherols were measured by fluorescence light detection (FLD) and compared with the retention time of commercial tocopherol standards.

Replicates of resulting pigment quantities were normalized to total pigment content, and tocopherols were normalized to total chlorophyll content in moles. All 188 replicates were screened for outliers using Cook's distance threshold of eight (Cook, 1977; Kim and Storer, 1996) which eliminated 17 replicates from downstream analyses. Variation in pigment and antioxidant relative abundances in all field and laboratory replicates was reduced to two dimensions using principal components analysis (PCA). Pigment and tocopherol data were then tested for normality with

the Shapiro–Wilk test (Shapiro and Wilk, 1965) prior to subsequent tests. The field site reference and lab-cultured plants were compared using the mean of HPLC biological replicates in a Mann–Whitney U-test (Mann and Whitney, 1947), and field treatments were compared with each other using the mean of HPLC biological replicates in paired Wilcoxon signed-rank tests (Wilcoxon, 1945) with BH adjustments. The pool size of viola-xanthin, antheraxanthin, and zeaxanthin (VAZ) was compared across field triplicates, with paired Wilcoxon signed-rank tests and multiple comparison adjustments as before.

Transcriptomics

To explore potential mechanisms of UV tolerance, transcript abundance was compared in field UV-filtered and UV-transmitted plants. Samples were collected in June 2019 from six window pairs (those which had sufficient tissue remaining after previous analyses) and stored dry, at room temperature in the dark until processing in July 2020. Stems were selected from each window sample, and dead tissue and debris were removed. Approximately 20 mg of dry weight per sample were placed into microcentrifuge tubes and sent to Novogene (Sacramento, CA, USA) for RNA extraction, library preparation, and transcriptome sequencing. Samples were processed according to the standard Novogene protocol, including preliminary quality check gel electrophoresis, quantitation, and purity assessment with NanoDrop (ThermoFisher Scientific, Waltham, MA, USA), and sample integrity assays with a Bioanalyzer 2100 (Agilent, Santa Clara, CA, USA). After quality checking procedures, oligo(dT) beads were used to enrich eukaryotic mRNA, and rRNA was removed with the Illumina Ribo-Zero kit (Illumina, Inc., San Diego, CA, USA). RNA samples were then reverse-transcribed into double-stranded cDNA libraries and sequenced on the 150 bp paired-end Illumina NovaSeq 6000 platform.

Transcriptome data were cleaned with Trimmomatic version 0.39 (Bolger et al., 2014) using a sliding window of 4 bp with a Phred quality score cut-off of 20, a minimum length of 20, and a leading and trailing minimum of three. The software packages Bowtie2 (Langmead and Salzberg, 2012) and Tophat2 (Kim et al., 2013) were used to make indexes of the reference S. caninervis genome (Silva et al., 2020) for mapping and assembly. Htseq-count version 0.9.1 (Anders et al., 2015) was used to estimate read counts per sample per gene, and final analyses were performed in R (R Core Team, 2019) using DESeq2 (Love et al., 2014) to test for differential transcript abundance in UV-filtered and UV-transmitted samples. To test for candidate genes associated with UV reduction and UV tolerance, transcript abundance was assessed with the DESeq2 formula: ~pair+window_treatment. In these comparisons, transcript counts were normalized with DESeq2's default model and significance was adjusted with the BH correction. For each comparison, transcripts were considered candidates for that effect if they had an absolute logarithmic (base 2) fold change (LFC) of at least 1 and an adjusted P-value (P-adj) of ≤0.005. Normalized transcript counts were log2-transformed and LFCs were shrunken with the approximate posterior estimation for the generalized linear model for plotting and ranking genes (Zhu et al., 2019). Variation in transcript abundances was reduced to two dimensions with

Table 1. Temperature in UV-filtered and UV-transmitted Mojave Desert microsites

		February	March	April	May	June	DF _n , DF _d	F	P-value
Mean daily low temperature (°C)	UV-filtered	-1.0±2.2	3.6±2.2	9.0±3.54	9.7±3.1	16.4±3.8	1, 28	0.004	NS
	UV-transmitted	-0.75±2.1	3.8±2.2	9.1±3.62	9.8±3.2	16.3±3.4			
Mean daily high temperature (°C)	UV-filtered	24.2±10.8	43.4±8.9	61.5±7.2	61.7±8.0	68.0±10.4	1, 28	0.006	NS
	UV-transmitted	23.8±10.7	43.4±8.6	61.4±7.0	61.0±7.9	66.9±9.6			

Mean \pm SD. P-values are reported for a one-way ANOVA with repeated measures; DF_n =degrees of freedom in the numerator, DF_d =degrees of freedom in the denominator, F=F-statistic, DF_d =not significant.

Results

Light measurements

PAR was measured in each field treatment to assess to what extent it is affected by the windows. There was no significant difference in PAR between UV-filtering and UV-transmitting windows. The mean PAR in UV-filtered plots was 1324 µmol m^{-2} s⁻¹ and the SD (σ) was 348 μ mol m⁻² s⁻¹. The mean PAR in UV-transmitted plots was 1343 μ mol m⁻² s⁻¹ (σ =340 μ mol m^{-2} s⁻¹). PAR in site reference sample sites (mean=1472 µmol m^{-2} s⁻¹, σ =345 μ mol m⁻² s⁻¹) was slightly but significantly higher than both UV-filtered and UV-transmitted windows (P=0.0002 and P=0.006, respectively). UV was significantly lower under UV-filtering windows relative to UV-transmitting windows (\sim 98% reduction from 91.3 μ mol m⁻² s⁻¹ to 1.6 μ mol m^{-2} s⁻¹; P < 0.0001, $\sigma = 25.5$ µmol m^{-2} s⁻¹ and 0.5 µmol m^{-2}

s⁻¹, respectively). Reference sites had higher UV than both UV-filtered and UV-transmitted sites (mean=105 umol m⁻² s^{-1} , σ =34.5 µmol m⁻² s⁻¹; P<0.0001 and P=0.001, respectively). Mean total light intensity of each treatment per month did not differ between the two windows (DF_n=1, DF_d=28, F=0.954, P=0.337).

Microclimate

Temperature and relative humidity were measured in order to test for the effects of UV-filtering and UV-transmitting windows on microclimate. Neither the mean daily low temperature per month nor the mean daily high temperature per month differed significantly between the UV-filtering and UV-transmitting windows over the 4 month monitoring period (Table 1).

Table 2. Relative humidity in UV-filtered, UV-transmitted, and site reference Mojave Desert microsites

		Site reference	UV-filtered	UV-transmitted	n	F	DF _n , DF _d	P-value
Winter	Mean daily low relative humidity (%)	NA	29.2±23.3	30.3±22.3	4	0.057	1, 22	NS
	Mean daily high relative humidity (%)	NA	100±0	88.9±8.8	4	2.306	1, 22	NS
Summer	Mean daily low relative humidity (%)	16.6±2.8	3.4±0.5	6.0±3.7	2	13.441	2, 3	0.032
	Mean daily high relative humidity (%)	56.8±5.3	36.2±22.9	36.9±23.9	2	0.727	2, 3	NS

Mean ±SD. P-values are reported for a one-way ANOVA with repeated measures; n=number of days, DF_n=degrees of freedom in the numerator, DF_d=degrees of freedom in the denominator, F=F-statistic, NS=not significant, NA=data not available.

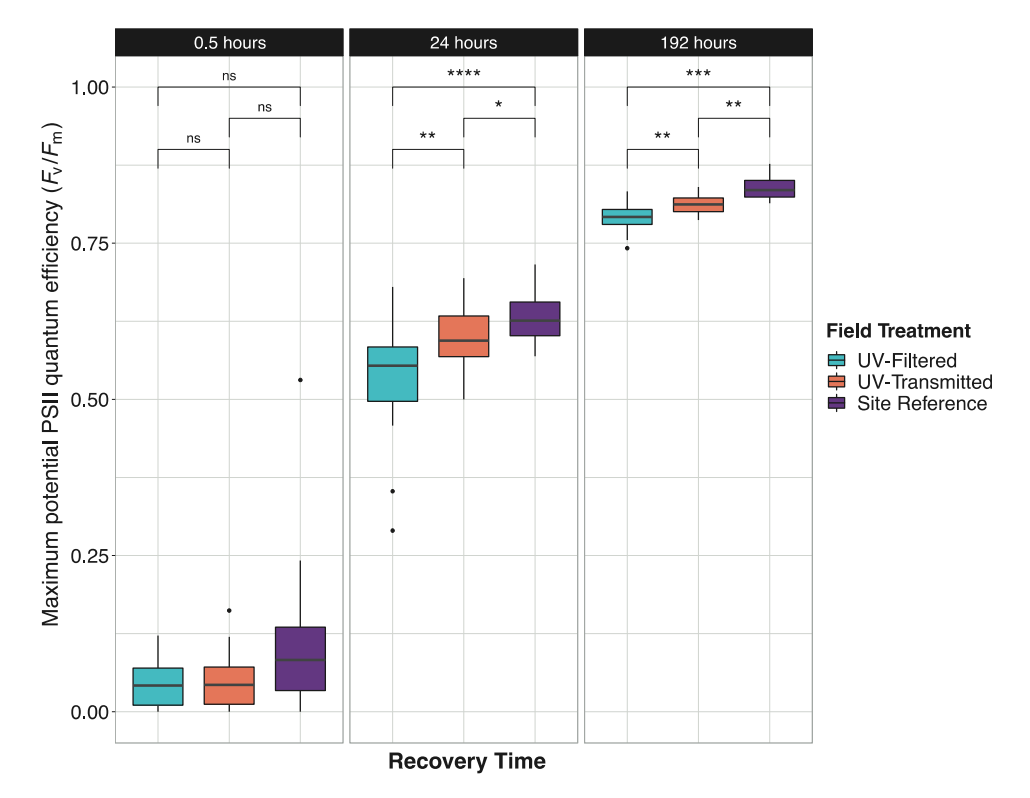


Fig. 3. Maximum potential PSII quantum efficiency of UV-filtered, UV-transmitted, and site reference Syntrichia caninervis over a simulated winter recovery period. F_v/F_m at each time point were compared pairwise using Wilcoxon signed-rank tests and adjusted for multiple testing with the Benjamini and Hochberg method. *P<0.05, **P<0.01, ***P<0.001, ****P<0.001.

4168 | Ekwealor et al.

Relative humidity was monitored in winter and summer. In the winter, the mean daily low and high relative humidity did not differ significantly between the two window treatments (Table 2). Summer microclimate monitoring included both treatment windows as well as nearby, unmanipulated site reference measurements. There was no significant difference in mean daily high relative humidity among the two treatment windows or site reference sample sites (Table 2). Treatment did have a significant effect on summer mean daily low relative humidity (Table 2); however, the post-hoc test found no significant differences in summer mean daily low relative humidity between UV-filtered and UV-transmitted windows. Summer daily low relative humidity was significantly higher in the site reference plot than in the UV-filtered window (adjusted P=0.033). It should be noted that relative humidity sensors are known to be unreliable at very high humidities and when wet. It is possible that some of the high relative humidity measurements recorded, especially those at 100% relative humidity, actually represent times when the sensors were wet from condensation.

Chlorophyll fluorescence of field-manipulated samples

 $F_{\rm v}/F_{\rm m}$ and $\Phi {\rm PSII}$ were measured at three time points over a simulated winter recovery period (192 h) to assess recovery of photosynthetic efficiency from desiccation. At T_{0.5}, rehydrated samples from all three field treatment groups had very low $F_{\rm v}/F_{\rm m}$ values (mean UV-filtered=0.044, σ =0.036; mean UV-transmitted=0.049, σ =0.045; and mean site reference=0.108, σ =0.122). There was no statistical difference in $F_{\rm v}/F_{\rm m}$ between any groups at $T_{0.5}$ (Fig. 3). After 24 h in simulated winter recovery conditions, $F_{\rm v}/F_{\rm m}$ had increased in all samples. At T_{24} , F_v/F_m of samples from UV-transmitting windows were significantly higher than those from UV-filtering (mean UV-filtered=0.532, σ =0.091; mean UV-transmitted=0.599, σ =0.054). Site reference samples had significantly higher F_v/F_m values (mean=0.631, σ =0.045) than UV-transmitted samples. At T_{192} , F_v/F_m values of all treatments were also significantly different from each other in the same rank order: UV-transmitted were higher than UV-filtered treatments, and site reference samples were higher than UV-transmitted treatments (mean UV-filtered=0.790,

Table 3. Mean quantum efficiency of PSII (Φ PSII) in UV-filtered and UV-transmitted *Syntrichia caninervis* plants over a simulated winter recovery period

Time in re- covery (h)	ΦPSII UV-filtered	ΦPSII UV-transmitted	n	<i>P</i> -adj
0	0.030±0.028	0.041±0.038	19	NS
24	0.329±0.061	0.389±0.060	19	0.001
192	0.584±0.037	0.606±0.032	19	0.003

Adjusted P-values are reported for Wilcoxon signed-rank tests with Benjamini and Hochberg correction. Mean \pm SD. n=number of pairs, NS=not significant.

 σ =0.023; mean UV-transmitted=0.812, σ =0.015; and mean site reference=0.839, σ =0.021). All treatment groups had relatively constant $F_{\rm o}$ over the simulated winter recovery period, while $F_{\rm m}$ increased from near 100 to at least 700 bits (Supplementary Fig. S3).

The pattern of Φ PSII measured at 150 µmol photons m⁻² s⁻¹ over the recovery period was similar to that of $F_{\rm v}/F_{\rm m}$. There was no statistical difference in Φ PSII between UV-filtered samples and UV-transmitted samples at T_{0.5} or between Φ PSII values of site reference plants and UV-transmitted plants (Table 3; Supplementary Fig. S2B). After 24 h in recovery, Φ PSII of all samples had increased. Φ PSII of samples from UV-transmitting windows were significantly higher than those from UV-filtering windows. Site reference mean Φ PSII was 0.425 (σ =0.044), and there was no significant difference between site reference and UV-transmitted samples. At T₁₉₂, neither UV-filtering and UV-transmitting, nor UV-transmitting and site reference Φ PSII values were significantly different from one another (site reference mean=0.630, σ =0.039).

Test for UV de-hardening at PSII

To test the hypothesis that UV filtering would de-harden plants and increase vulnerability to UV damage at PSII, desiccated plants from all three field treatments were subjected to a laboratory UV treatment, and $F_{\rm v}/F_{\rm m}$ and Φ PSII were measured during simulated winter recovery conditions. There were no significant differences in $F_{\rm v}/F_{\rm m}$ within each treatment group (UV-filtered, UV-transmitted, and site reference) at $T_{0.5}$ and T_{192} after the laboratory UV treatment (Supplementary Fig. S2A). At T_{24} , UV-transmitted field plants that received a laboratory UV treatment had significantly higher $F_{\rm v}/F_{\rm m}$ than UV-transmitted plants that did not. Similarly, Φ PSII of each treatment group was not significantly different after the laboratory UV treatment at $T_{0.5}$ and T_{192} , but at T_{24} was significantly higher in laboratory UV-treated UV-transmitted samples with no laboratory UV treatment (Fig. S2B).

Photosynthesis pigment and antioxidant content

Photosynthesis pigments and antioxidants were measured in field-collected plants from all treatments as well as in lab-cultured plants. Zeaxanthin levels and the Chl a:b ratio increased with UV filtering, while neoxanthin and Chl b decreased (Fig. 4). Unmanipulated site reference samples also had significantly more zeaxanthin, lutein, β -carotene, and a higher Chl a:b ratio, as well as lower violaxanthin, neoxanthin, Chl a, and Chl b than UV-transmitted samples. There was no significant difference in violaxanthin, antheraxanthin, lutein, β -carotene, or Chl a between UV-filtered samples and UV-transmitted samples, though the VAZ pool was larger in UV-filtered plants than in UV-transmitted plants (P=0.048).

The three field treatment groups (UV-filtered, UV-transmitted, and site reference) and the laboratory cultures

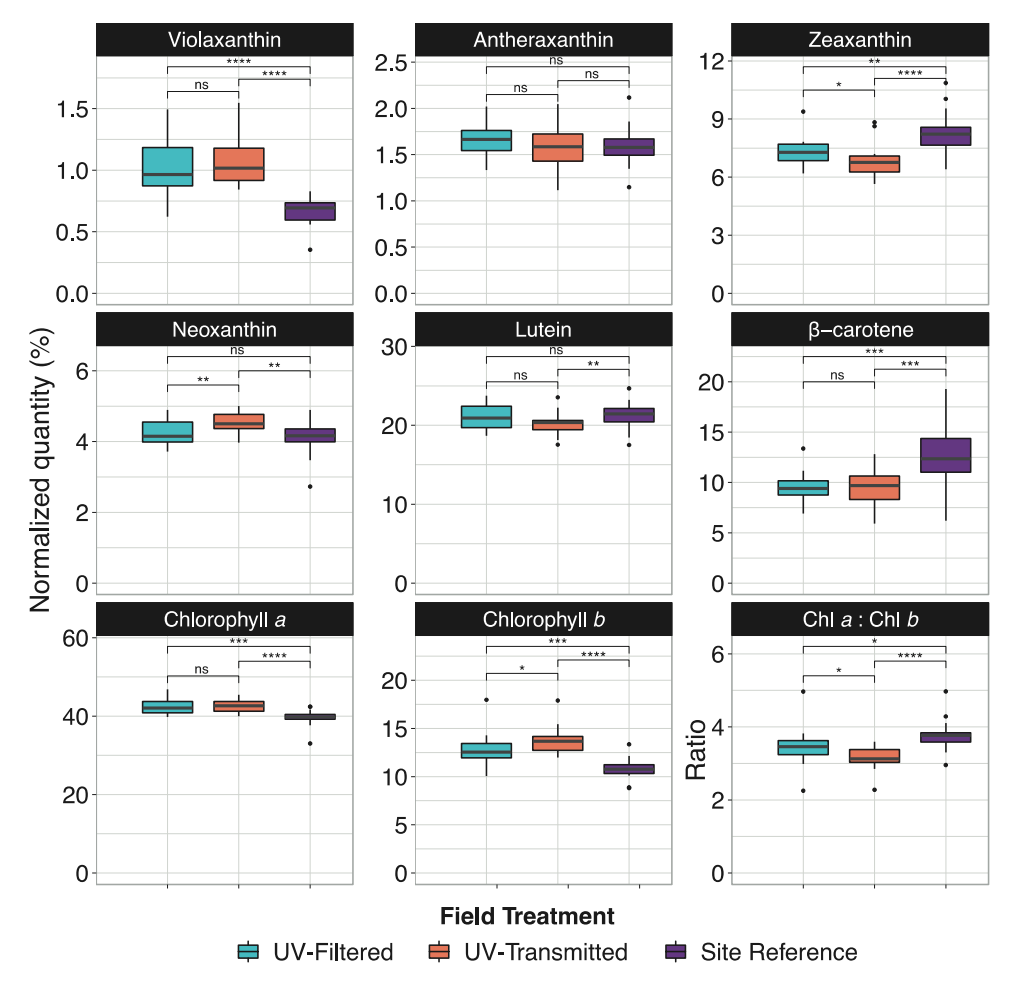


Fig. 4. Relative content of photosynthetic pigments in UV-filtered, UV-transmitted, and site reference Syntrichia caninervis. Pigment and antioxidant content were quantified by HPLC in at least triplicate and normalized to total pigment content by moles. Means were compared across field treatments using Wilcoxon signed-rank tests with the Benjamini and Hochberg correction for multiple tests. *P<0.05, **P<0.01, ***P<0.001, ****P<0.0001.

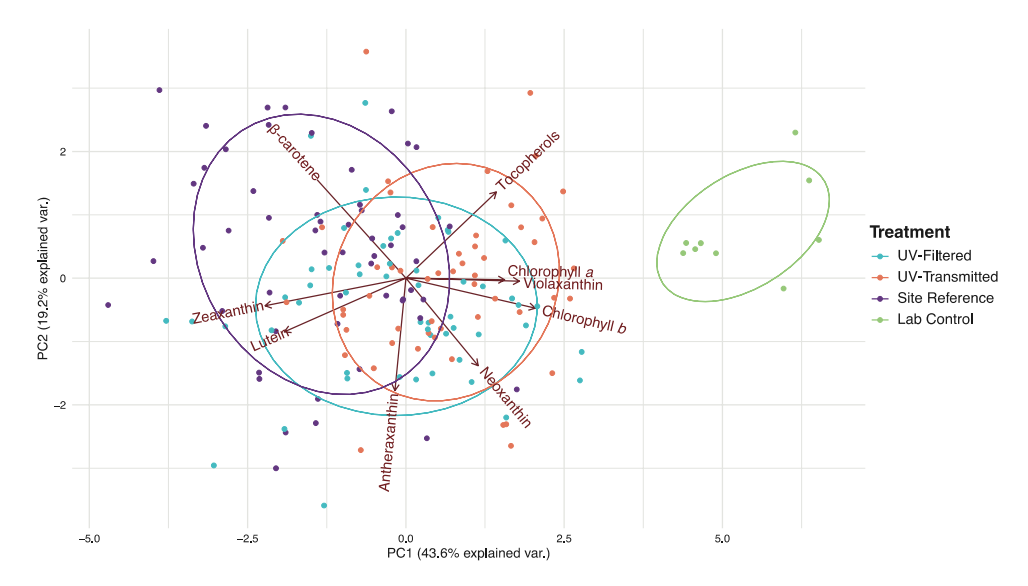


Fig. 5. Principal components biplot of first and second PCA scores based on relative photosynthesis pigment and tocopherol content in UV-filtered, UV-transmitted, unaltered field-collected (site reference), and laboratory-cultured Syntrichia caninervis. Vectors are overlaid and scaled to show the strength of correlation. Composition 68% probability ellipses show the means (ellipse centers) and variation by treatment. Pigment and antioxidant contents were quantified by HPLC in at least triplicate and normalized to total pigment content. Replicates were screened for outliers.

Table 4. Mean relative abundance of photosynthesis pigments in field-collected and laboratory-cultured *Syntrichia caninervis* plants

	Field- collected (% of total pigment in mol)	Lab- cultured (% of total pigment in mol)	$n_{\rm F}, n_{ m L}$	<i>P</i> -adj
Violaxanthin	0.661±0.172	4.42±0.819	61, 9	<0.0001
Antheraxanthin	1.59±0.294	1.53±0.317	61, 9	NS
Zeaxanthin	8.33±1.33	1.55±0.331	61, 9	< 0.0001
Neoxanthin	4.12±0.699	4.81±0.333	61, 9	0.0005
Lutein	21.4±2.54	17.9±1.14	61, 9	< 0.0001
β-Carotene	12.6±4.20	8.42±1.62	61, 9	0.002
Chl a	39.7±4.37	42.8±2.27	61, 9	0.024
Chl b	10.8±2.01	18.6±0.696	61, 9	< 0.0001

Adjusted P-values are reported for Wilcoxon tests with Benjamini and Hochberg correction. Mean \pm SD. n_F =number of field-collected replicates, n_I =number of lab-cultured replicates, NS=not significant.

Table 5. Mean relative abundance of tocopherols in UV-filtered and UV-transmitted *Syntrichia caninervis* plants

	UV-filtered (mmol mol ⁻¹)	UV-transmitted (mmol mol ⁻¹)	n	<i>P</i> -adj
α-Tocopherol	16.7±3.59	14.7±3.43	19	0.026
β-Tocopherol	5.69±1.58	4.17±1.54	19	0.002

Adjusted P-values reported are for Wilcoxon signed-rank tests with Benjamini and Hochberg correction. Data normalized by Chl a. Mean \pm SD. n=number of pairs.

separated along PCA axis PC1, which explained 43.6% of the variation (Fig. 5). The field treatments were largely overlapping with each other, and the laboratory cultures were relatively distant. Field-collected site reference plants had a lower proportion of Chl a, Chl b, violaxanthin, and neoxanthin than lab-cultured plants (Table 4). The field-collected plants also had more zeaxanthin, lutein, and β -carotene than lab-cultured plants (Table 4). There was no significant difference in antheraxanthin abundance between site reference and lab-cultured plants.

Normalized α - and β -tocopherols increased with removal of UV (Table 5). Site reference samples had higher α - and β -tocopherols than UV-transmitted samples (Fig. 6). Field-collected plants had a much higher relative abundance of α - and β -tocopherols than lab-cultured plants (Table 6).

Transcriptomics

Differential transcript abundance analyses performed on six pairs of field-manipulated samples (UV-filtered and UV-transmitted) revealed a total of 6885 genes in the 12 transcriptomes. In the transcript PCA, the two field treatments (UV-filtered and UV-transmitted) did not separate along PC1, which explained 41% of the variation, nor along PC2, which explained 24% (Fig. 7). However, the pairs tended to cluster near each other along these two PC axes. After filtering for an absolute LFC of at least one, 19 genes were identified as significantly differentially abundant between field treatments (*P*-adj <0.005; Table 7; Fig. 8).

Discussion

F_v/F_m recovery

Field-collected S. caninervis plants from all treatments had very low maximum potential PSII quantum efficiency, $F_{\rm v}/F_{\rm m}$, when initially rehydrated, but recovered over 8 d in simulated winter conditions in which $F_{\rm v}/F_{\rm m}$ increased from <0.1 to 0.81. In unstressed land plants, $F_{\rm v}/F_{\rm m}$ is nearly constant around 0.83 (Björkman and Demmig, 1987; Proctor, 2001). Often a low F_v/F_m is assumed to indicate stress related to PSII damage primarily attributed to inactivation of the core reaction center D1-protein (Demmig and Björkman, 1987; Csintalan et al., 1999), and thus increasing F_v/F_m is interpreted as repair of PSII as part of the D1 cycle (Melis, 1999). However, because $F_{\rm v}/F_{\rm m}$ is a normalized ratio, it is important to determine which component is driving $F_{\rm v}/F_{\rm m}$ depression or recovery. As $F_v = F_m - F_o$, F_v / F_m is equivalent to $(F_{\rm m}-F_{\rm o})/F_{\rm m}$, and the ratio can increase over time (i.e. during recovery) due to increasing $F_{\rm m}$ or decreasing $F_{\rm o}$, or both. Understanding change in these variables over time can provide insight into the underlying biological processes contributing to observed change in $F_{\rm v}/F_{\rm m}$. For example, $F_{\rm o}$ is high when PSII is damaged (Rintamäki et al., 1994; Ritchie, 2006; Murchie and Lawson, 2013). An increase in F_v/F_m due to a decrease in F_0 with a relatively constant F_m would be strongly indicative of PSII damage and subsequent repair. On the other hand, an increase in $F_{\rm v}/F_{\rm m}$ driven by rising $F_{\rm m}$ is consistent with a relaxation of NPQ (Müller et al., 2001). This latter scenario is what we observed in S. caninervis recovering from $F_{\rm v}/F_{\rm m}$ depression: an increase in $F_{\rm v}/F_{\rm m}$ over the recovery period driven by $F_{\rm m}$, which suggests relaxation of sustained NPQ rather than repair of damaged or inactivated PSII (Supplementary Fig. S3).

Different pigment and antioxidant profiles in fieldcollected and lab-cultured plants

Comparison of the photosynthetic pigment profiles in fieldcollected and lab-cultured S. caninervis supports this hypothesis of relaxation of sustained NPQ. Zeaxanthin, which is associated with both rapidly reversible (qE) and sustained NPQ mechanisms such as photoinhibitory quenching (qI; Demmig-Adams, 1990; Verhoeven et al., 1996), was more than five times higher in field-collected plants than in lab-cultured plants (Table 4). In fact, the relative VAZ pool was larger in field-collected plants, which is unsurprising as these pigments increase in abundance in high-light environments (Siefermann-Harms, 1985; Demmig-Adams, 1990; Jahns et al., 2009). Zeaxanthin accumulation is associated with sustained NPQ in desiccation-tolerant mosses, specifically accumulating when desiccation occurs in natural light conditions (Verhoeven et al., 2020). The higher levels of zeaxanthin in field-collected plants suggest accumulation due to the desiccation in the natural habitat but not in the laboratory cultures. Similarly, in field-collected plants, the proportion of chlorophyll of the total pigment content was reduced and

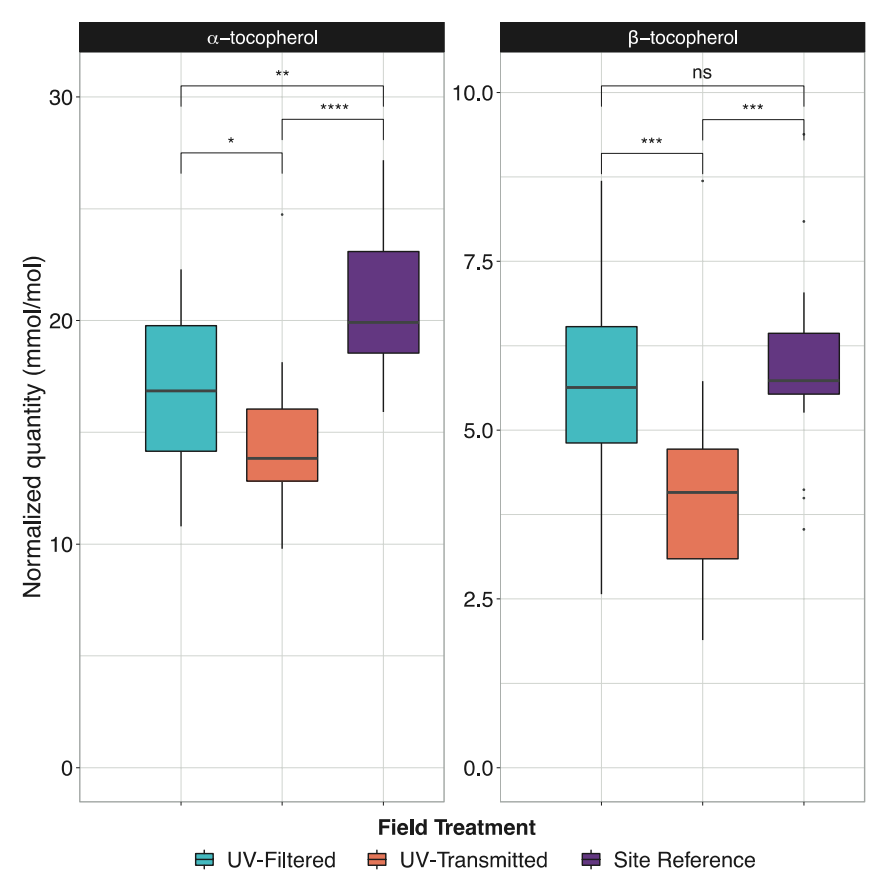


Fig. 6. Relative tocopherol content in UV-filtered, UV-transmitted, and unaltered site reference Syntrichia caninervis. Tocopherol content was quantified by HPLC in at least triplicate and normalized to total chlorophyll content. Means were compared across field treatments using Wilcoxon signed-rank tests with the Benjamini and Hochberg correction for multiple tests. *P<0.05, **P<0.01, ***P<0.001, ****P<0.0001.

Table 6. Mean relative abundance of tocopherols in fieldcollected and laboratory-cultured Syntrichia caninervis plants

	Field-collected (mmol mol ⁻¹)	Lab-cultured (mmol mol ⁻¹)	n _F , `n _L	P-adj
α-Tocopherol	20.6±6.27	9.56±3.08	61, 9	<0.0001
β-Tocopherol	5.95±2.21	1.28±0.764	61, 9	< 0.0001

Adjusted P-values are reported for Wilcoxon tests with Benjamini and Hochberg correction. Data normalized by Chl a. Mean \pm SD. $n_{\rm F}$ =number of field-collected replicates, n_1 =number of lab-cultured replicates.

the Chl a:b ratio was increased, also consistent with acclimation to high-light intensity (Björkman, 1981; Leong and Anderson, 1984; Lindahl et al., 1995). Tocopherol abundance was also much higher in field-collected plants than in those cultured in the lab (Table 6). Tocopherols are membrane-bound phenolic antioxidants that may be increased due to the higher light intensity and UV exposure in the field site (Delong and Steffen, 1998; Yao et al., 2015) or due to other stresses such as desiccation and freezing that these plants frequently face in their natural habitat (Munné-Bosch, 2005).

Altered F₁/F_m recovery following UV filtering

Surprisingly, F_v/F_m was not affected in rehydrated S. caninervis when natural levels of UV were reduced for 1 year, but the recovery of $F_{\rm v}/F_{\rm m}$ was impaired during at least 192 h in winter recovery conditions (Fig. 3). In contrast, many plants respond to supplemental UV radiation with reduced F_v/F_m (Bradshaw, 1965; Strid et al., 1990; He et al., 1993; Pukacki and Modrzyński, 1998; Ranjbarfordoei et al., 2011; but see Takács et al., 1999; Csintalan et al., 2001; Lau et al., 2006; Basahi et al., 2014). Furthermore, the relative abundance of the xanthophyll zeaxanthin was also increased in UV-filtered plants (Fig. 4), a response also typically seen with UV supplementation (Agrawal et al., 2009). Why should removal of UV radiation, presumably a stressor, result in altered recovery of F_v/F_m and more antioxidant xanthophylls in S. caninervis? One possible explanation for the observed reduction in $F_{\rm v}/F_{\rm m}$ recovery is that removal of UV somehow causes an impairment in relaxation of sustained NPQ. As with unmanipulated field-collected plants, the observed $F_{\rm v}/F_{\rm m}$ increase over the recovery period for UV-filtered and UV-transmitted plants was driven by an increase in $F_{\rm m}$ and

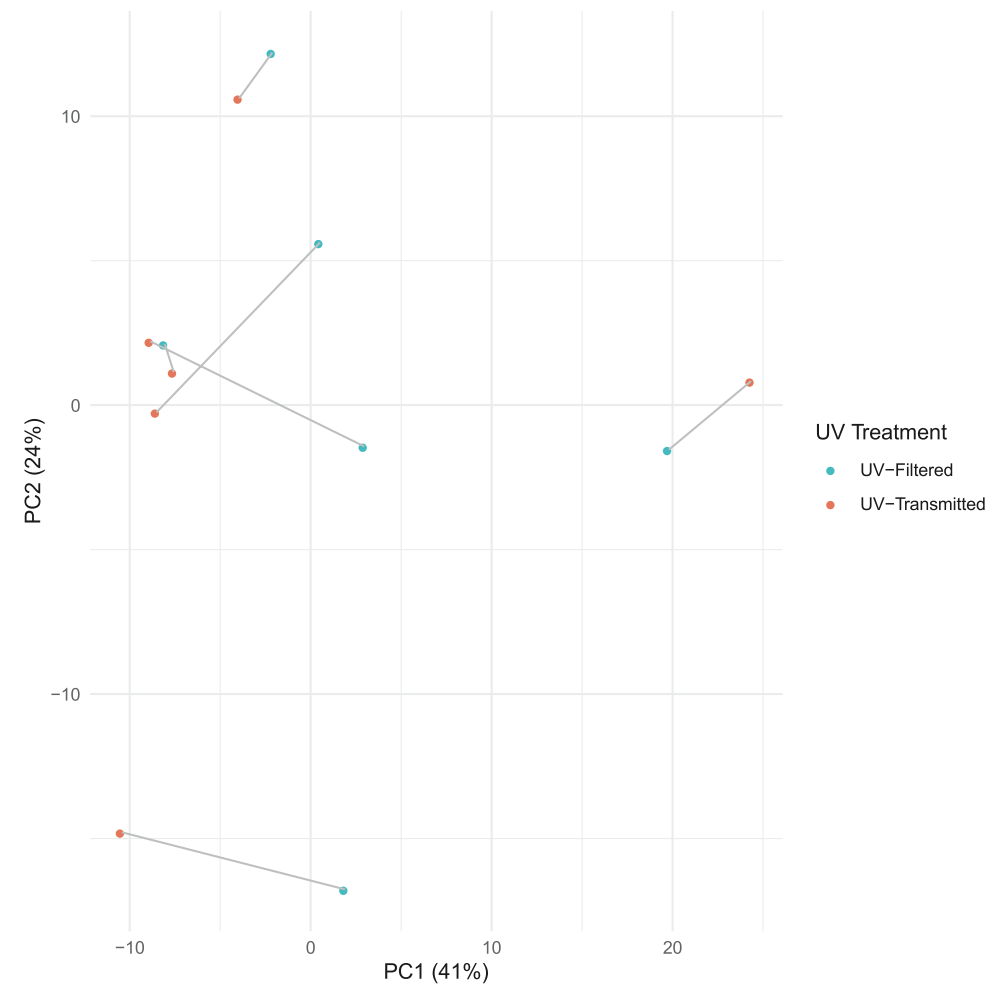


Fig. 7. Principal components biplot of first and second PCA scores based on normalized transcript counts for six field-manipulated microsite pairs (UV-filtered and UV-transmitted) of Syntrichia caninervis. Lines connect pairs from each of the six collection sites in the paired design.

thus is consistent with relaxation of sustained NPQ. Indeed, the increased abundance of zeaxanthin with removal of UV is consistent with the hypothesis that UV filtering induces a sustained zeaxanthin-related NPQ (Verhoeven et al., 1996). Although zeaxanthin is not required for sustained quenching, its accumulation probably contributes to sustained NPQ when present (Verhoeven et al., 2020).

It is possible that UV radiation is a photomorphogenic (Gitz and Liu-Gitz, 2003) or regulatory signal rather than (or in addition to) being a stressor, such that the absence of this signal indirectly affects $F_{\rm v}/F_{\rm m}$ recovery (Hideg et al., 2013). For example, UV may induce production of enzymatic antioxidants or phenolics (Cooper-Driver et al., 1998; Clarke and Robinson, 2008; Waterman et al., 2017) that may have roles beyond UV protection, such as in desiccation tolerance (Gitz and Liu-Gitz, 2003; Poulson et al., 2006; Robson et al., 2015). Without these UV-associated responses, desiccation in the field might cause more photo-oxidative stress. In addition to increased VAZ pool size, the relative abundance of tocopherols increased with removal of UV from S. caninervis in the field (Fig. 6; Table 5), suggestive of increased ROS activity. Tocopherols quench singlet oxygen from the PSII reaction center (Trebst et al., 2002; Trebst, 2003; Krieger-Liszkay, 2005), and α-tocopherol has been shown to confer antioxidant protection to thylakoid membranes in UV-B-exposed spinach plants (Delong and Steffen, 1998). There are a number of stress protection mechanisms mediated by UVR8, the UV-B-sensing protein receptor (Singh et al., 2014), many of which could result in slower F_v/F_m recovery and increased antioxidant abundance without UV-induced signaling. In fact, the UV-B response pathway and the photomorphogenesis pathway have substantial overlap (Stanley and Yuan, 2019).

Transcriptomic response to reduced UV

Transcriptomic profiling of the UV-filtered and UV-transmitted plants revealed an altered transcript abundance of genes involved in flavonoid biosynthesis and essential plant function. Commonly located in vacuoles or cell walls, flavonoids are phenolic secondary metabolic compounds important for

Table 7. Putative function and Gene Ontology (GO) terms for the differentially abundant transcripts with UV filtering in wild Syntrichia caninervis

Gene	GO terms			LFC	Stat	P-adj
	Cellular components	Molecular functions	Biological processes			
Sc_g01390: alpha-xylosidase 1-like		Hydrolase activity, hydrolyzing O-glycosyl compounds, carbohydrate binding	Carbohydrate metabolic process	1.48	5.34	0.00021
Sc_g07909: omega-6 fatty acid desaturase, chloroplastic	Integral com- ponent of membrane		Lipid metabolic process	1.20	4.35	0.00497
Sc_g06438: prolyl endopeptidase isoform X2		Serine-type endopeptidase activity, serine-type exopeptidase	Proteolysis	1.19	5.13	0.00037
Sc_g07907: acyl-lipid (9-3)-desaturase-like	Integral com- ponent of	Oxidoreductase activity, metal ion binding	Unsaturated fatty acid biosynthetic process, oxidation—reduction process	1.06	4.78	0.00131
Sc_g1598: mechanosensitive ion channel protein 1, mitochondrial-like Sc_g15405: probable aquaporin PIP2-8	Membrane Integral component of	Channel activity	Transmembrane transport	0.90	-5.16 4.76	0.00037
Sc_g13500: potassium transporter 5-like	Integral component of membrane	Potassium ion transmembrane transporter activity	Potassium ion transmem- brane transport	0.79	4.66	0.00182
Sc_g13420; protein EFFECTOR OF TRANSCRIPTION 2-like		DNA binding	Regulation of transcription, DNA-templated	-0.77	4.66	0.00182
Sc_g05612: beta-galactosidase 8-like isoform X1		β-Galactosidase activity	Carbohydrate metabolic	0.77	5.08	0.00037
Sc_g08662: alpha-xylosidase 1-like		Hydrolase activity, hydrolyzing O-glycosyl compounds, carbohy- drate binding	Carbohydrate metabolic process	92.0	4.45	0.00369
Sc_g10528: glutamine synthetase cytosolic isozyme		Glutamate-ammonia ligase activity, ATP binding	Glutamine biosynthetic process	0.75	4.47	0.00350
Sc_g11712: light-inducible protein CPRF2		DNA-binding transcription factor activity	Regulation of transcription, DNA-templated	-0.62	-6.19	0.00000
Sc_g07665; ABC transporter G family member 38-like	Integral component of membrane	ATP binding, ATPase activity		0.55	4.55	0.00266
Sc_g15028: antifreeze protein Sc_g11402: probable polyamine oxidase 2	Peroxisome	Polyamine oxidase activity	Polyamine catabolic process, oxidation-reduction process	0.54	5.11	0.00234
Sc_g15925; probable protein phosphatase 2C 15 isoform X1		Protein serine/threonine phosphatase activity	Protein dephosphorylation	0.51	2.00	0.00049
Sc_g07772: phosphoenolpyruvate carboxylase 2	Cytosol, chloroplast, apoplast		Tricarboxylic acid cycle, carbon fixation, leaf devel- coment	-0.41	4.36	0.00497
Sc_g09506: carbonic anhydrase, chloroplastic-like	Cytoplasm	Channel activity	Response to carbon dioxide, regulation of stomatal movement, carbon utilization	-0.36	-6.02	0.00001
Sc_g13890: dihydrolipoyllysine-residue acetyltransferase component 5 of pyruvate dehydrogenase complex, chloroplastic		Protein serine/threonine phosphatase activity		0.31	5.00	0.00497

Adjusted P-values reported for Wald tests with Benjamini and Hochberg correction. LFC=log2 fold change with UV-transmitted as the reference (+ LFC indicates an increase in abundance with UV filtering); Stat=Wald statistic.

Downloaded from https://academic.oup.com/jxb/article/72/11/4161/6141413 by University of California School of Law (Boalt Hall) user on 25 May 2021

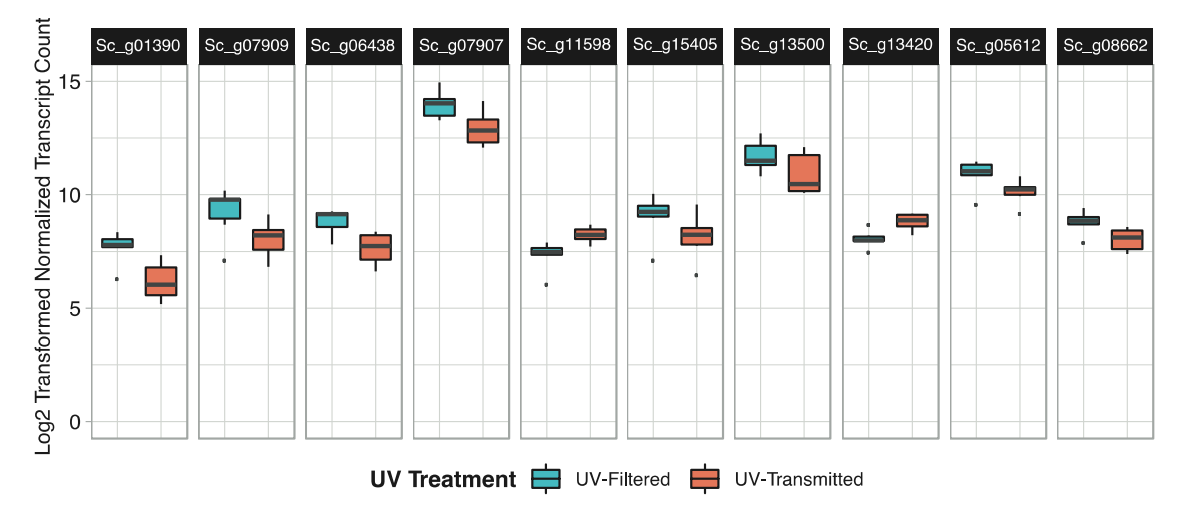


Fig. 8. Normalized transcript counts of the top 10 most differentially abundant (P<0.005) transcripts with UV filtering in field-treated Syntrichia caninervis.

tolerance to UV (e.g. via antioxidant function or UV absorption) and a variety of other stresses in plants (Cooper-Driver et al., 1998; Graham, 1998; Markham et al., 1998; Grace and Logan, 2000; Wolf et al., 2010). Two of the 19 differentially abundant transcripts, including the most differentially abundant transcript, were for the α-xylosidase 1-like genes, Sc_ g01390 and Sc_g08662, which were nearly 1.5 and 0.76 log2-fold higher, respectively, with UV filtering. A glycoside hydrolase, α-xylosidase 1-like, may be involved in the breakdown of flavonol glycosides, as glycosylation is necessary for stable flavonoid accumulation in other plants (Luo et al., 2007; Lee et al., 2017). In both rice and Arabidopsis thaliana, the abundance of flavonol glycosides including kaempferol and quercetin glycosides increases with UV-B radiation (Graham, 1998; Markham et al., 1998; Veit and Pauli, 1999). Correspondingly, glycosyl hydrolase transcript abundance decreases with UV-B exposure in Artemisia annua, suggesting inhibition of breakdown (Pan et al., 2014). In contrast, we found increased abundance of glycoside hydrolase α-xylosidase 1-like transcripts with UV filtering in S. caninervis, suggesting increased glycoside breakdown and reduced glycoside accumulation, which may negatively affect UV tolerance. Similarly, transcripts of the gene Sc_g05612, β-galactosidase 8-like isoform X1, increased with UV filtering and also codes for a glycoside hydrolase and may be involved in inhibition of flavonoid biosynthesis. Importantly in A. thaliana, β -galactosidase has been shown to increase in activity during drought- and senescence-induced photoinhibition (Mohapatra et al., 2010; Pandey et al., 2017), a form of photosynthetic down-regulation.

Two genes associated with oxidoreductase activity, Sc_g11402, probable polyamine oxidase 2; and Sc_g07907, acyl-lipid (9-3)-desaturase-like, significantly increased in abundance with UV filtering in *S. caninervis*. Polyamine oxidases are involved in ROS homeostasis in *A. thaliana*, and some are up-regulated by drought stress in *A. thaliana* and the resurrection plant *Craterostigma plantagineum* (Alcázar *et al.*, 2011; Andronis *et al.*,

2014). Increased abundance of these transcripts with UV filtering may suggest increased oxidative stress with UV removal.

In addition to being involved in oxidoreductase activity, the fatty acid desaturase Sc g07907, acyl-lipid (9-3)-desaturase, is involved in biosynthesis of fatty acids such as gamma linolenic acid (Sayanova et al., 1997). Linolenic acid is a critical player in maintenance of membrane integrity and functionality of membrane proteins, including photosynthetic machinery proteins (Upchurch, 2008). Along with the second most differentially abundant transcript (Sc_g07909: omega-6 fatty acid desaturase, chloroplastic), the increased abundance of these two fatty acid biosynthetic pathway genes suggests biosynthesis or repair of membranes, perhaps chloroplast membranes, with UV filtering in S. caninervis. In fact, lipid hydroperoxidation of membranes is a major form of ROS damage (Foyer et al., 1994; Alscher et al., 1997; Shigeoka et al., 2002) Together, differential abundance of transcripts involved in oxidative stress and membrane biosynthesis supports our hypothesis that removal of natural levels of UV radiation can lead to oxidative stress in S. caninervis.

Laboratory UV treatment of field-treated samples

In our study, application of an additional UV treatment to field window samples had no significant effect on $F_{\rm v}/F_{\rm m}$ of UV-filtered plants over the 192 h simulated winter recovery period (Supplementary Fig. S2). This result suggests either that the 1 year of reduced UV in the field was not sufficient to remove previously acquired acclimation or that these plants may have a physiologically constitutive level of protection in this assay. However, the mechanism of protection in the UV-filtered and UV-transmitted plants might have been different, as there were differences in their pigment and antioxidant profiles. For example, zeaxanthin was higher in UV-filtered plants and zeaxanthin has been found to contribute to UV stress protection and UV damage prevention in tobacco plants (Götz *et al.*, 2002). It is also possible that any PSII damage incurred by the

UV treatment was repaired in the 30 min dark acclimation period prior to the first fluorescence measurement. Curiously, UV-transmitted plants had significantly higher F_v/F_m at T_{24} after the laboratory UV treatment, and UV-filtered plants showed the same pattern, though it was not significant. This result lends further support to the hypothesis that UV exposure has beneficial effects on photosynthetic efficiency in S. caninervis following desiccation, as even a moderate dose of UV applied to these desiccated mosses improved $F_{\rm v}/F_{\rm m}$ recovery.

Conclusions

In summary, we find evidence that Mojave Desert S. caninervis plants undergo a sustained form of NPQ that takes days to relax and for efficient photosynthesis to resume in simulated winter conditions. As these plants spend much of the summer season in a dry, quiescent state under extremes in PAR and UV exposure, the 8 d F_v/F_m recovery we observed suggests strong recovery potential which may be mediated by seasonal photoprotective thermal dissipation (Demmig-Adams et al., 2012). Furthermore, reduction of UV radiation from natural sunlight had unexpected and adverse effects on recovery of photosynthetic efficiency in S. caninervis following rehydration. This counterintuitive finding is consistent with photoinhibitory effects from heightened levels of singlet oxygen and other ROS, and may be driven by exposure to high visible light in the absence of a UV regulatory signal that probably induces multiple protective responses. Evidence to support this hypothesis includes the three photoprotective response metrics we observed in our UV-filtered plants: significantly higher zeaxanthin and tocopherols—both potential antioxidants—and increased abundance of transcripts associated with oxidative stress. Yet, all field plants in this study had high levels of these antioxidants, which, along with the chlorophyll fluorescence results, suggests that they undergo a strong and sustained form of NPQ, which in this system takes as long as 8 d post-rehydration before highly efficient photosynthesis can resume. It is difficult to distinguish PSII damage due to ROS in the presence of sustained NPQ and it is possible that UV-reduced plants have higher NPQ. More research is needed to determine to what extent these two processes, ROS damage and sustained NPQ, are contributing to the observed altered recovery of F_v/F_m in UV-reduced plants, and how these factors interact with desiccation in natural populations.

Supplementary data

The following supplementary data are available at *IXB* online. Fig. S1. Modified 24-well plates known as 'water thrones' described in Clark (2020), which allow mosses to remain hydrated and near 100% relative humidity through a water-wicking system.

Fig. S2. Mean maximum potential PSII quantum efficiency and PSII operating quantum efficiency ±SE of UV-filtered, UV-transmitted, and site reference plants over a simulated winter recovery period, with and without a laboratory UV treatment.

Fig. S3. Baseline (F_0) and maximum (F_m) fluorescence of UV-filtered, UV-transmitted, and site reference plants over a simulated winter recovery period.

Acknowledgements

The authors would like to thank Carl J. Rothfels, Kirsten K. Coe, and Ben K. Blackman for their feedback on earlier versions of this manuscript. We also thank Cindy V. Looy, Ivo A.P. Duijnstee, and Jeffrey P. Benca for their assistance with measuring UV-B flux from our experimental lamps. This work was supported by the University of California, Berkeley, Department of Integrative Biology Graduate Research Fund to JTBE; the UC Natural Reserve System Mildred E. Mathias Research Grant to JTBE; the American Bryological and Lichenological Society Anderson & Crum Field Research Award to JTBE; German Research Foundation (DFG) project number 427925948 to OD; and National Science Foundation Dimensions of Biodiversity awards (DEB-1638956 and DEB 1638943) to BDM and LRS, respectively. KKN is an investigator of the Howard Hughes Medical Institute. JTBE was also supported by the University of California Berkeley Fellowship, the UC Berkeley Pinto-Fialon Fellowship, and the National Science Foundation Dimensions of Biodiversity award (DEB-1638956).

Author contributions

JTBE, BDM, and TAC conceptualized the research. JTBE performed field investigation. JTBE, OD, AR, TAC, and SE performed the laboratory investigation. JTBE and OD performed formal analyses and all authors interpreted them. JTBE wrote the original draft and all authors contributed to review and editing.

Data availability

The data that support these findings are openly available on GitHub at: https://github.com/jenna-tb-ekwealor/syntrichia_field_UV.

References

Agrawal SB, Singh S, Agrawal M. 2009. Ultraviolet-B induced changes in gene expression and antioxidants in plants. Advances in Botanical Research **52**, 47-86.

Alcázar R, Bitrián M, Bartels D, Koncz C, Altabella T, Tiburcio AF. 2011. Polyamine metabolic canalization in response to drought stress in Arabidopsis and the resurrection plant Craterostigma plantagineum. Plant Signaling & Behavior 6, 243-250.

Alscher RG, Donahue JL, Cramer CL. 1997. Reactive oxygen species and antioxidants: relationships in green cells. Physiologia Plantarum 100,

Anders S, Pyl PT, Huber W. 2015. HTSeq-a Python framework to work with high-throughput sequencing data. Bioinformatics 31, 166-169.

Andronis EA, Moschou PN, Toumi I, Roubelakis-Angelakis KA. 2014. Peroxisomal polyamine oxidase and NADPH-oxidase cross-talk for ROS homeostasis which affects respiration rate in Arabidopsis thaliana. Frontiers in Plant Science 5, 132.

Antoninka A, Bowker MA, Reed SC, Doherty K. 2016. Production of greenhouse-grown biocrust mosses and associated cyanobacteria to rehabilitate dryland soil function. Restoration Ecology 24, 324–335.

Baroli I. Nivogi KK. 2000. Molecular genetics of xanthophyll-dependent photoprotection in green algae and plants. Philosophical Transactions of the Royal Society B: Biological Sciences 355, 1385-1394.

Basahi JM, Ismail IM, Hassan IA. 2014. Effects of enhanced UV-B radiation and drought stress on photosynthetic performance of lettuce (Lactuca sativa L. Romaine) plants. Annual Research & Review in Biology **4**, 1739-1756.

Belnap J. 2002. Nitrogen fixation in biological soil crusts from southeast Utah, USA. Biology and Fertility of Soils 35, 128-135.

Belnap J. 2006. The potential roles of biological soil crusts in dryland hydrologic cycles. Hydrological Processes 20, 3159-3178.

Belnap J, Hawkes CV, Firestone MK. 2003. Boundaries in miniature: two examples from soil. BioScience 53, 739-749.

Benjamini Y, Hochberg Y. 1995. Controlling the false discovery rate: a practical and powerful approach to multiple testing. Journal of the Royal Statistical Society: Series B (Methodological) 57, 289–300.

Björkman O. 1981. Responses to different quantum flux densities. In: Lange OL, Nobel PS, Osmond CB, Ziegler H, eds. Physiological plant ecology I. New York: Springer-Verlag, 57-108.

Björkman O, Demmig B. 1987. Photon yield of O₂ evolution and chlorophyll fluorescence characteristics at 77 K among vascular plants of diverse origins. Planta 170, 489-504.

Björn LO. 2007. Stratospheric ozone, ultraviolet radiation, and cryptogams. Biological Conservation 135, 326-333.

Boelen P, De Boer MK, De Bakker NVJ, Rozema J. 2006. Outdoor studies on the effects of solar UV-B on bryophytes: overview and methodology. Plant Ecology 182, 137-152.

Bolger AM, Lohse M, Usadel B. 2014. Trimmomatic: a flexible trimmer for illumina sequence data. Bioinformatics 30, 2114-2120.

Bowker MA, Stark LR, McLetchie DN, Mishler BD. 2000. Sex expression, skewed sex ratios, and microhabitat distribution in the dioecious desert moss Syntrichia caninervis (Pottiaceae). American Journal of Botany **87**, 517-526.

Bradshaw AD. 1965. Evolutionary significance of phenotypic plasticity in plants. Advances in Genetics 13, 115-155.

Clark TA. 2020. Can desert mosses hide from climate change? The ecophysiological importance of habitat buffering & water relations to a keystone biocrust moss in the Moiave Desert, PhD thesis, University of Nevada.

Clarke LJ. Robinson SA. 2008. Cell wall-bound ultraviolet-screening compounds explain the high ultraviolet tolerance of the Antarctic moss, Ceratodon purpureus. New Phytologist 179, 776-783.

Coe KK, Belnap J, Sparks JP, 2012. Precipitation-driven carbon balance controls survivorship of desert biocrust mosses. Ecology 93, 1626-1636.

Cook RD. 1977. Detection of influential observation in linear regression. Technometrics 19, 15-18.

Cooper-Driver GA, Bhattacharya M, Harborne JB. 1998. Role of phenolics in plant evolution. Phytochemistry 49, 1165-1174.

Csintalan Z, Proctor MCF, Tuba Z. 1999. Chlorophyll fluorescence during drying and rehydration in the mosses Rhytidiadelphus loreus (Hedw.) Warnst., Anomodon viticulosus (Hedw.) Hook. and Tayl. and Grimmia pulvinata (Hedw.) Sm. Annals of Botany 84, 235-244.

Csintalan Z, Tuba Z, Takács Z, Laitat E. 2001. Responses of nine bryophyte and one lichen species from different microhabitats to elevated UV-B radiation. Photosynthetica 39, 317-320.

Dautermann O. Lyska D. Andersen-Ranberg J. et al. 2020. An algal enzyme required for biosynthesis of the most abundant marine carotenoids. Science Advances 6, eaaw9183.

Davey MP, Susanti NI, Wargent JJ, Findlay JE, Paul Quick W, Paul ND, Jenkins Gl. 2012. The UV-B photoreceptor UVR8 promotes photosynthetic efficiency in Arabidopsis thaliana exposed to elevated levels of UV-B. Photosynthesis Research 114, 121-131.

Delong JM, Steffen KL. 1998. Lipid peroxidation and α -tocopherol content in α -tocopherol-supplemented thylakoid membranes during UV-B exposure. Environmental and Experimental Botany 39, 177-185.

Demmia B. Biörkman O. 1987. Comparison of the effect of excessive light on chlorophyll fluorescence (77K) and photon yield of O2 evolution in leaves of higher plants. Planta 171, 171-184.

Demmig-Adams B. 1990. Carotenoids and photoprotection in plants: a role for the xanthophyll zeaxanthin. Biochima et Biophysica Acta 1020,

Demmig-Adams B, Adams WW. 1996. Xanthophyll cycle and light stress in nature: uniform response to excess direct sunlight among higher plant species, Planta 198, 460-470.

Demmig-Adams B, Cohu CM, Muller O, Adams WW 3rd. 2012. Modulation of photosynthetic energy conversion efficiency in nature: from seconds to seasons. Photosynthesis Research 113, 75-88.

Dunn JL, Robinson SA. 2006. Ultraviolet B screening potential is higher in two cosmopolitan moss species than in a co-occurring Antarctic endemic moss: implications of continuing ozone depletion. Global Change Biology 12, 2282-2296.

Ekwealor JTB. 2020. A suntan effect in the Mojave Desert moss Syntrichia caninervis 2020, 15-18. https://granite.ucnrs.org/wp-content/ uploads/2021/02/2020_Science-Newsletter.pdf.

Ekwealor JTB, Fisher KM. 2020. Life under quartz: hypolithic mosses in the Mojave desert. PLoS One 15, e0235928.

Foyer CH, Descourvieres P, Kunert KJ. 1994. Protection against oxygen radicals: an important defence mechanism studied in transgenic plants. Plant, Cell & Environment 17, 507-523.

Frohnmeyer H, Staiger D. 2003. Ultraviolet-B radiation-mediated responses in plants. Balancing damage and protection. Plant Physiology 133, 1420-1428

Gaff DF. 1977. Desiccation tolerant vascular plants of southern Africa. Oecologia 31, 95-109.

Gitz DC, Liu-Gitz L. 2003. How do UV photomorphogenic responses confer water stress tolerance? Photochemistry and Photobiology 78, 529-534.

Götz T, Sandmann G, Römer S. 2002. Expression of a bacterial carotene hydroxylase gene (crtZ) enhances UV tolerance in tobacco. Plant Molecular Biology 50, 129-142.

Grace SC, Logan BA. 2000. Energy dissipation and radical scavenging by the plant phenylpropanoid pathway. Philosophical Transactions of the Royal Society B; Biological Sciences 355, 1499–1510.

Graham TL. 1998. Flavonoid and flavonol glycoside metabolism in Arabidopsis. Plant Physiology and Biochemistry 36, 135-144.

Green TGAA, Kulle D, Pannewitz S, Sancho LG, Schroeter B. 2005. UV-A protection in mosses growing in continental Antarctica. Polar Biology **28**. 822-827.

Grolemund G, Wickham H. 2011. Dates and times made easy with {lubridate}. Journal of Statistical Software 40, 1-25.

Gwynn-Jones D, Lee JA, Johanson U, Phoenix GK, Callaghan TV, Sonesson M. 1999. The response of plant functional types to enhanced UV-B radiation. In: Rozema J, ed. Stratospheric ozone depletion: the effects of enhanced UV-B radiation on terrestrial ecosystems. Swedish Polar Research Secretariat, Abisko Scientific Research Station, 173–186.

Harper KT, Belnap J. 2001. The influence of biological soil crusts on mineral uptake by associated vascular plants. Journal of Arid Environments 47, 347-357.

Hawkes CV. 2004. Effects of biological soil crusts on seed germination of four endangered herbs in a xeric Florida shrubland during drought. Plant Ecology **170**, 121–134.

He J, Huang L, Chow W, Whitecross M, Anderson J. 1993. Effects of supplementary ultraviolet-B radiation on rice and pea plants. Functional Plant Biology 20, 129-142.

Hespanhol H, Fabón G, Monforte L, Martínez-Abaigar J, Núñez-Olivera E. 2014. Among- and within-genus variability of the UV-absorption capacity in saxicolous mosses. The Bryologist 117, 1-9.

Hideg É, Jansen MAK, Strid Å. 2013. UV-B exposure, ROS, and stress: inseparable companions or loosely linked associates? Trends in Plant Science 18, 107-115.

Hoadland DR. Arnon DI. 1950. The water-culture method for growing plants without soil. Circular 347. California Agricultural Experiment Station.

Hope RM. 2013. Rmisc. https://cran.r-project.org/web/packages/Rmisc/

Horton P, Ruban AV, Walters RG. 1996. Regulation of light harvesting in green plants. Annual Review of Plant Physiology and Plant Molecular Biology 47, 655-684.

Hutin C, Nussaume L, Moise N, Moya I, Kloppstech K, Havaux M. 2003. Early light-induced proteins protect Arabidopsis from photooxidative stress. Proceedings of the National Academy of Sciences, USA 100,

Jafari M. Ansari-Pour N. 2019. Why, when and how to adjust your P values? Cell Journal 20, 604-607.

Jahns P. Latowski D. Strzalka K. 2009. Mechanism and regulation of the violaxanthin cycle: the role of antenna proteins and membrane lipids. Biochimica et Biophysica Acta 1787, 3-14.

Jansen MAK, Gaba V, Greenberg BM. 1998. Higher plants and UV-B radiation: balancing damage, repair and acclimation. Trends in Plant Science **3**, 131–135.

Jasoni RL, Smith SD, Arnone JA. 2005. Net ecosystem CO2 exchange in Mojave Desert shrublands during the eighth year of exposure to elevated CO₂. Global Change Biology **11**, 749–756.

Jeffree CE. 2007. The fine structure of the plant cuticle. In: Riederer M. Müller C, eds. Annual plant reviews: biology of the plant cuticle. Oxford: Blackwell Publishing, 11-25.

Kassambara A. 2020a. rstatix: pipe-friendly framework for basic statistical tests. https://cran.r-project.org/web/packages/rstatix/index.html

Kassambara A. 2020b. ggpubr: 'ggplot2' based publication ready plots. https://cloud.r-project.org/web/packages/ggpubr/index.html

Kim C. Storer BE. 1996. Reference values for Cook's distance. Communications in Statistics Part B: Simulation and Computation 25, 691-708.

Kim D, Pertea G, Trapnell C, Pimentel H, Kelley R, Salzberg SL. 2013. TopHat2: accurate alignment of transcriptomes in the presence of insertions, deletions and gene fusions. Genome Biology 14, R36.

Krieger-Liszkay A. 2005. Singlet oxygen production in photosynthesis. Journal of Experimental Botany 56, 337-346.

Langmead B. Salzberg SL. 2012. Fast gapped-read alignment with Bowtie 2. Nature Methods 9, 357-359.

Lau TSL, Eno E, Goldstein G, Smith C, Christopher DA. 2006. Ambient levels of UV-B in Hawaii combined with nutrient deficiency decrease photosynthesis in near-isogenic maize lines varying in leaf flavonoids: flavonoids decrease photoinhibition in plants exposed to UV-B. Photosynthetica 44, 394-403.

Lee YS, Woo JB, Ryu SI, Moon SK, Han NS, Lee SB. 2017. Glucosylation of flavonol and flavanones by Bacillus cyclodextrin glucosyltransferase to enhance their solubility and stability. Food Chemistry 229, 75-83.

Leong TY, Anderson JM. 1984. Adaptation of the thylakoid membranes of pea chloroplasts to light intensities. I. Study on the distribution of chlorophyll-protein complexes. Photosynthesis Research 5, 105-115.

Li XR, Jia XH, Long LQ, Zerbe S. 2005. Effects of biological soil crusts on seed bank, germination and establishment of two annual plant species in the Tengger Desert (N China). Plant and Soil 277, 375–385.

Li Z, Wakao S, Fischer BB, Niyogi KK. 2009. Sensing and responding to excess light. Annual Review of Plant Biology 60, 239-260.

Liquori N. Xu P. van Stokkum IHM. van Oort B. Lu Y. Karcher D. Bock R, Croce R. 2017. Different carotenoid conformations have distinct functions in light-harvesting regulation in plants. Nature Communications

Lindahl M, Yang DH, Andersson B. 1995. Regulatory proteolysis of the major light-harvesting chlorophyll a/b protein of photosystem II by a light-induced membrane-associated enzymic system. European Journal of Biochemistry 231, 503-509.

Love MI, Huber W, Anders S. 2014. Moderated estimation of fold change and dispersion for RNA-seg data with DESeg2. Genome Biology 15, 550.

Lud D, Moerdijk TCW, Van de Poll WH, Buma AGJ, Huiskes AHL. 2002. DNA damage and photosynthesis in Antarctic and Arctic Sanionia uncinata (Hedw.) Loeske under ambient and enhanced levels of UV-B radiation, Plant, Cell & Environment 25, 1579-1589.

Luo J, Nishiyama Y, Fuell C, et al. 2007. Convergent evolution in the BAHD family of acyl transferases: identification and characterization of anthocyanin acyl transferases from Arabidopsis thaliana. The Plant Journal **50**. 678-695.

Malnoë A. 2018. Photoinhibition or photoprotection of photosynthesis? Update on the (newly termed) sustained quenching component qH. Environmental and Experimental Botany 154, 123-133.

Mann HB, Whitney DR. 1947. On a test of whether one of two random variables is stochastically larger than the other. Annals of Mathematical Statistics 18, 50-60.

Markham KR. Tanner GJ. Caasi-Lit M. Whitecross MI. Navudu M. Mitchell KA. 1998. Possible protective role for 3',4'-dihydroxyflavones induced by enhanced UV-B in a UV-tolerant rice cultivar. Phytochemistry 49, 1913-1919

Martínez-Abaigar J, Núñez-Olivera E, Beaucourt N, García-Álvaro MA, Tomás R, Arróniz M. 2003. Different physiological responses of two aquatic bryophytes to enhanced ultraviolet-B radiation. Journal of Bryology 25, 17-30.

Melis A. 1999. Photosystem-II damage and repair cycle in chloroplasts: what modulates the rate of photodamage? Trends in Plant Science 4,

Middleton EM, Teramura AH. 1993. The role of flavonol glycosides and carotenoids in protecting soybean from ultraviolet-B damage. Plant Physiology 103, 741-752.

Middleton N, Thomas DSG. 1992. World atlas of desertification. London: Edward Arnold.

Mohapatra PK, Patro L, Raval MK, Ramaswamy NK, Biswal UC, Biswal B. 2010. Senescence-induced loss in photosynthesis enhances cell wall beta-glucosidase activity. Physiologia Plantarum 138, 346-355.

Morales LO, Brosché M, Vainonen J, Jenkins GI, Wargent JJ, Sipari N, Strid Å, Lindfors AV, Tegelberg R, Aphalo PJ. 2013. Multiple roles for UV RESISTANCE LOCUS8 in regulating gene expression and metabolite accumulation in Arabidopsis under solar ultraviolet radiation. Plant Physiology 161, 744-759.

Müller P, Li XP, Niyogi KK. 2001. Non-photochemical quenching. A response to excess light energy. Plant Physiology 125, 1558-1566.

Munné-Bosch S. 2005. The role of alpha-tocopherol in plant stress tolerance. Journal of Plant Physiology 162, 743-748.

Murchie EH, Lawson T. 2013. Chlorophyll fluorescence analysis: a guide to good practice and understanding some new applications. Journal of Experimental Botany 64, 3983-3998.

Neugart S, Schreiner M. 2018. UVB and UVA as eustressors in horticultural and agricultural crops. Scientia Horticulturae 234, 370-381.

Newsham KK. 2003. UV-B radiation arising from stratospheric ozone depletion influences the pigmentation of the Antarctic moss Andreaea regularis. Oecologia 135, 327-331.

Niyogi KK. 2000. Safety valves for photosynthesis. Current Opinion in Plant Biology 3, 455-460.

Núñez-Olivera E, Arróniz-Crespo M, Martínez-Abaigar J, Tomás R, Beaucourt N. 2005. Assessing the UV-B tolerance of sun and shade samples of two aquatic bryophytes using short-term tests. The Bryologist 108, 435-448

Oliver MJ, Dowd SE, Zaragoza J, Mauget SA, Payton PR. 2004. The rehydration transcriptome of the desiccation-tolerant bryophyte Tortula ruralis: transcript classification and analysis. BMC Genomics 5, 89.

Pan WS, Zheng LP, Tian H, Li WY, Wang JW. 2014. Transcriptome responses involved in artemisinin production in Artemisia annua L. under UV-B radiation. Journal of Photochemistry and Photobiology. B, Biology 140, 292-300

Pandey JK, Dash SK, Biswal B. 2017. Loss in photosynthesis during senescence is accompanied by an increase in the activity of β-galactosidase in leaves of Arabidopsis thaliana: modulation of the enzyme activity by water stress. Protoplasma 254, 1651-1659.

Peel MC, Finlayson BL, Mcmahon TA. 2007. Updated world Koppen-Geiger climate classification map. Hydrology and Earth System Sciences **11**. 1633-1644.

Poulson ME, Boeger MR, Donahue RA. 2006. Response of photosynthesis to high light and drought for Arabidopsis thaliana grown under a UV-B enhanced light regime. Photosynthesis Research 90, 79-90.

Proctor M. 2001. Patterns of desiccation tolerance and recovery in bryophytes. Plant Growth Regulation 35, 147-156.

Proctor MCF, Oliver MJ, Wood AJ, Alpert P, Stark LR, Cleavitt NL, Mishler BD. 2007. Desiccation-tolerance in bryophytes: a review. The Bryologist 110, 595-621.

Pukacki PM. Modrzyński J. 1998. The influence of ultraviolet-B radiation on the growth, pigment production and chlorophyll fluorescence of Norway spruce seedlings. Acta Physiologiae Plantarum 20, 245-250.

Ranjbarfordoei A, Samson R, Van Damme P. 2011. Photosynthesis performance in sweet almond Prunus dulcis (Mill) D. Webb] exposed to supplemental UV-B radiation. Photosynthetica 49, 107-111.

R Core Team. 2019. R: a language and environment for statistical computing. Vienna, Austria: R Foundation for Statistical Computing.

Rintamäki E, Salo R, Aro E-M. 1994. Rapid turnover of the D1 reactioncenter protein of photosystem II as a protection mechanism against photoinhibition in a moss, Ceratodon purpureus (Hedw.) Brid. Planta 193,

Ritchie GA. 2006. Chlorophyll fluorescence: what is it and what do the numbers mean? USDA Forest Service Proceedings RMRS-P-43,

Robinson SA, Turnbull JD, Lovelock CE. 2005. Impact of changes in natural ultraviolet radiation on pigment composition, physiological and morphological characteristics of the Antarctic moss, Grimmia antarctici. Global Change Biology 11, 476-489.

Robson TM, Hartikainen SM, Aphalo PJ. 2015. How does solar ultraviolet-B radiation improve drought tolerance of silver birch (Betula pendula Roth.) seedlings? Plant, Cell & Environment 38, 953-967.

Rozema J, van de Staaij J, Björn LO, Caldwell M. 1997. UV-B as an environmental factor in plant life: stress and regulation. Trends in Ecology & Evolution 12, 22-28.

Ruban AV. 2016. Nonphotochemical chlorophyll fluorescence guenching: mechanism and effectiveness in protecting plants from photodamage. Plant Physiology 170, 1903-1916.

Sayanova O, Smith MA, Lapinskas P, Stobart AK, Dobson G, Christie WW, Shewry PR, Napier JA. 1997. Expression of a borage desaturase cDNA containing an N-terminal cytochrome b5 domain results in the accumulation of high levels of $\Delta 6$ -desaturated fatty acids in transgenic tobacco. Proceedings of the National Academy of Sciences, USA 94,

Searles PS, Flint SD, Caldwell MM. 2001. A meta-analysis of plant field studies simulating stratospheric ozone depletion. Oecologia 127, 1-10.

Searles PS, Flint SD, Díaz SB, Rousseaux MC, Ballaré CL, Caldwell MM. 1999. Solar ultraviolet-B radiation influence on Sphagnum bog and Carex fen ecosystems: first field season findings in Tierra del Fuego, Argentina. Global Change Biology 5, 225–234.

Seppelt RD, Downing AJ, Deane-Coe KK, Zhang Y, Zhang J. 2016. Bryophytes within biological soil crusts. In: Weber B, Büdel B, Belnap J, eds. Biological soil crusts: an organizing principle in drylands. Ecological Studies Vol. 226. Cham: Springer, 101–120.

Shapiro SS, Wilk MB. 1965. An analysis of variance test for normality (complete samples). Biometrika 52, 591-611.

Shigeoka S, Ishikawa T, Tamoi M, Miyagawa Y, Takeda T, Yabuta Y, Yoshimura K. 2002. Regulation and function of ascorbate peroxidase isoenzymes. Journal of Experimental Botany 53, 1305-1319.

Siefermann-Harms D. 1985. Carotenoids in photosynthesis. I. Location in photosynthetic membranes and light-harvesting function. Biochimica et Biophysica Acta 811, 325-355.

Silva AT, Gao B, Fisher KM, et al. 2020. To dry perchance to live: insights from the genome of the desiccation-tolerant biocrust moss Syntrichia caninervis. The Plant Journal doi: 10.1111/tpj.15116.

Singh S, Agrawal SB, Agrawal M. 2014. UVR8 mediated plant protective responses under low UV-B radiation leading to photosynthetic acclimation. Journal of Photochemistry and Photobiology B: Biology 137, 67-76.

Stanley L. Yuan YW. 2019. Transcriptional regulation of carotenoid biosynthesis in plants: so many regulators, so little consensus. Frontiers in Plant Science 10, 1017.

Stark LR. 2005. Phenology of patch hydration, patch temperature and sexual reproductive output over a four-year period in the desert moss Crossidium crassinerve. Journal of Bryology 27, 231-240.

Stark LR. 2017. Ecology of desiccation tolerance in bryophytes: a conceptual framework and methodology. The Bryologist 120, 130-165.

Stark LR, Mishler BD, McLetchie DN. 1998. Sex expression and growth rates in natural populations of the desert soil crustal moss Syntrichia caninervis. Journal of Arid Environments 40, 401-416.

Strid Å, Chow WS, Anderson JM. 1990. Effects of supplementary ultraviolet-B radiation on photosynthesis in Pisum sativum. Biochimica et Biophysica Acta 1020, 260-268.

Su Y-G, Li X-R, Cheng Y-W, Tan H-J, Jia R-L. 2007. Effects of biological soil crusts on emergence of desert vascular plants in North China. Plant Ecology **191**, 11–19.

Takács Z, Csintalan Z, Sass L, Laitat E, Vass I, Tuba Z. 1999. UV-B tolerance of bryophyte species with different degrees of desiccation tolerance. Journal of Photochemistry and Photobiology B: Biology 48, 210-215.

Teramura AH, Sullivan JH. 1994. Effects of UV-B radiation on photosynthesis and growth of terrestrial plants. Photosynthesis Research 39,

Tohge T, Fernie AR. 2017. Leveraging natural variance towards enhanced understanding of phytochemical sunscreens. Trends in Plant Science 22, 308-315.

Trebst A. 2003. Function of β-carotene and tocopherol in photosystem II. Zeitschrift fur Naturforschung - Section C Journal of Biosciences 58,

Trebst A, Depka B, Holländer-Czytko H. 2002. A specific role for tocopherol and of chemical singlet oxygen quenchers in the maintenance of photosystem II structure and function in Chlamydomonas reinhardtii. FEBS Letters **516**. 156–160.

Tukey JW. 1949. Comparing individual means in the analysis of variance. Biometrics 5, 99-114.

Turnbull JD, Leslie SJ, Robinson SA. 2009. Desiccation protects two Antarctic mosses from ultraviolet-B induced DNA damage. Functional Plant Biology 36, 214-221.

Upchurch RG. 2008. Fatty acid unsaturation, mobilization, and regulation in the response of plants to stress. Biotechnology Letters 30, 967–977.

VanBuren R, Pardo J, Man Wai C, Evans S, Bartels D. 2019. Massive tandem proliferation of ELIPs supports convergent evolution of desiccation tolerance across land plants. Plant Physiology 179, 1040-1049.

Veit M, Pauli GF. 1999. Major flavonoids from Arabidopsis thaliana leaves. Journal of Natural Products 62, 1301-1303.

Verhoeven AS, Adams WW, Demmig-Adams B. 1996. Close relationship between the state of the xanthophyll cycle pigments and photosystem Il efficiency during recovery from winter stress. Physiologia Plantarum 96, 567-576.

Verhoeven AS, Berkowitz JM, Walton BN, Berube BK, Willour JJ, Polich SB. 2020. Is zeaxanthin needed for desiccation tolerance? Sustained forms of thermal dissipation in tolerant versus sensitive bryophytes. Physiologia Plantarum doi: 10.1111/ppl.13263.

Vu VQ. 2011. ggbiplot: a ggplot2 based biplot. https://www.rdocumentation. org/packages/ggbiplot/versions/0.55

Waterman MJ, Nugraha AS, Hendra R, Ball GE, Robinson SA, Keller PA. 2017. Antarctic moss biflavonoids show high antioxidant and ultraviolet-screening activity. Journal of Natural Products 80, 2224-2231.

Wickham H. 2016. ggplot2: elegant graphics for data analysis. New York: Springer-Verlag

Wickham H. Averick M. Brvan J. et al. 2019. Welcome to the {tidvverse}. Journal of Open Source Software 4, 1686

Wickham H, François R, Henry L, Müller K. 2020. dplyr: a grammar of data manipulation. https://dplyr.tidyverse.org/reference/dplyr-package.html

Wilcoxon F. 1945. Individual comparisons by ranking methods. Biometrics Bulletin 1, 80-83.

Williamson CE, Zepp RG, Lucas RM, et al. 2014. Solar ultraviolet radiation in a changing climate. Nature Climate Change 4, 434-441.

Wolf L, Rizzini L, Stracke R, Ulm R, Rensing SA. 2010. The molecular and physiological responses of Physcomitrella patens to ultraviolet-B radiation. Plant Physiology 153, 1123-1134.

Yamakawa H, Fukushima Y, Itoh S, Heber U. 2012. Three different mechanisms of energy dissipation of a desiccation-tolerant moss serve one common purpose: to protect reaction centres against photo-oxidation. Journal of Experimental Botany 63, 3765-3775.

Yamakawa H, Itoh S. 2013. Dissipation of excess excitation energy by drought-induced nonphotochemical quenching in two species of droughttolerant moss: desiccation-induced acceleration of photosystem II fluorescence decay. Biochemistry 52, 4451-4459.

Yao Y, You J, Ou Y, Ma J, Wu X, Xu G. 2015. Ultraviolet-B protection of ascorbate and tocopherol in plants related with their function on the stability on carotenoid and phenylpropanoid compounds. Plant Physiology and Biochemistry 90, 23-31.

Zaady E. Kuhn U. Wilske B. Sandoval-Soto L. Kesselmeier J. 2000. Patterns of CO₂ exchange in biological soil crusts of successional age. Soil Biology and Biochemistry 32, 959-966.

Zeng Q. Chen X. Wood AJ. 2002. Two early light-inducible protein (ELIP) cDNAs from the resurrection plant Tortula ruralis are differentially expressed in response to desiccation, rehydration, salinity, and high light. Journal of Experimental Botany 53, 1197-1205.

Zhu A, Ibrahim JG, Love MI. 2019. Heavy-tailed prior distributions for sequence count data: removing the noise and preserving large differences. Bioinformatics 35, 2084-2092.

Zotz G, Kahler H. 2007. A moss 'canopy'-small-scale differences in microclimate and physiological traits in Tortula ruralis. Flora 202, 661-666.